Available online at www.sciencedirect.com

ScienceDirect

Geochimica et Cosmochimica Acta 206 (2017) 166–183

Geochimica et Cosmochimica Acta

www.elsevier.com/locate/gca

Hydrogen isotopes of *n*-alkanes and *n*-alkanoic acids as tracers of precipitation in a temperate forest and implications for paleorecords

Erika J. Freimuth *, Aaron F. Diefendorf, Thomas V. Lowell

Department of Geology, University of Cincinnati, PO Box 210013, Cincinnati, OH 45221-0013, USA

Received 5 July 2016; accepted in revised form 20 February 2017; Available online 27 February 2017

Abstract

The hydrogen isotopic composition of leaf waxes (δD_{wax}) primarily reflects that of plant source water. Therefore, sedimentary δD_{wax} records are increasingly used to reconstruct the δD of past precipitation (δD_p) and to investigate paleohydrologic changes. Such reconstructions rely on estimates of apparent fractionation (ε_{app}) between δD_p and the resulting δD_{wax}. However, ε_{app} values are modified by numerous environmental and biological factors during leaf wax production. As a result, ε_{app} can vary widely among plant species and growth forms. This complicates estimation of accurate ε_{app} values and presents a central challenge to quantitative leaf wax paleohydrology. During the 2014 growing season, we examined ε_{app} in the five deciduous angiosperm tree species (*Prunus serotina*, *Acer saccharinum*, *Quercus rubra*, *Quercus alba*, and *Ulmus americana*) that dominate the temperate forest at Brown's Lake Bog, Ohio, USA. We sampled individuals of each species at weekly to monthly intervals from March to October and report δD values of *n*-C_{29} alkanes ($\delta D_{n\text{-C29 alkane}}$) and *n*-$C_{28}$ alkanoic acids ($\delta D_{n\text{-C28 acid}}$), as well as xylem ($\delta D_{xw}$) and leaf water ($\delta D_{lw}$). *n*-Alkane synthesis was most intense 2–3 weeks after leaf emergence and ceased thereafter, whereas *n*-alkanoic acid synthesis continued throughout the entire growing season. During bud swell and leaf emergence, δD_{lw} was a primary control on $\delta D_{n\text{-C29 alkane}}$ and $\delta D_{n\text{-C28 acid}}$ values, which stabilized once leaves became fully expanded. Metabolic shifts between young and mature leaves may be an important secondary driver of δD_{wax} changes during leaf development. In mature autumn leaves of all species, the mean ε_{app} for *n*-C_{29} alkane (−107‰) was offset by approximately −19‰ from the mean ε_{app} for *n*-C_{28} alkanoic acid (−88‰). These results indicate that in temperate settings *n*-alkanes and *n*-alkanoic acids from deciduous trees are distinct with respect to their abundance, timing of synthesis, and ε_{app} values.

Keywords: Paleohydrology; Leaf wax; Hydrogen isotope; Apparent fractionation; Angiosperms

1. INTRODUCTION

The hydrogen isotope composition (δD) of precipitation is governed by isotope effects during hydrologic processes (Craig, 1961). Plants synthesize leaf waxes using hydrogen derived from plant source waters (including soil, stream and lake water), which are fed by precipitation. Therefore, the hydrogen isotopic composition of leaf waxes (δD_{wax}) primarily reflects that of local precipitation (δD_p) both in modern plants (Sachse et al., 2006; Smith and Freeman, 2006; Tipple and Pagani, 2013; Feakins et al., 2016) and in sediments (Sachse et al., 2004; Hou et al., 2008; Polissar and Freeman, 2010; Sachse et al., 2012). Thus, δD_{wax} from lacustrine and marine sediments has been used to investigate paleohydrology throughout the Cenozoic (Pagani et al., 2006; Tierney et al., 2008; Rach et al., 2014). The net offset between sedimentary δD_{wax} (measured) and past δD_p (calculated) is known as apparent

* Corresponding author.
E-mail address: erika.freimuth@gmail.com (E.J. Freimuth).

http://dx.doi.org/10.1016/j.gca.2017.02.027
0016-7037/

fractionation (ε_{app}). Estimates of ε_{app} are therefore critical for accurate δD_p reconstruction. However, ε_{app} remains the largest source of uncertainty in leaf wax paleohydrology (Sachse et al., 2012; Polissar and D'Andrea, 2014).

ε_{app} values are influenced by a suite of environmental and biological factors. For example, deuterium (D)-enrichment of the biosynthetic water pool from which lipids are synthesized can be driven by soil evaporation (McInerney et al., 2011) and leaf transpiration (Feakins and Sessions, 2010; Sachse et al., 2010; Kahmen et al., 2013b). In addition, leaf wax biosynthesis results in considerable D-depletion of the wax product relative to the biosynthetic water pool from which it is synthesized (Sachse et al., 2012). This δD offset is known as biosynthetic fractionation (ε_{bio}). Some evidence suggests that ε_{bio} is constant within a species (Sessions et al., 1999; Tipple et al., 2015) while other studies have found that ε_{bio} may vary throughout the growing season (Newberry et al., 2015; Sachse et al., 2015). Among species, ε_{bio} can vary by up to 65‰ (Kahmen et al., 2013b). This may contribute to considerable interspecies ε_{app} differences of up to 65‰ among species in a temperate deciduous forest (Hou et al., 2007), 99‰ in an arid shrub ecosystem (Feakins and Sessions, 2010) and 109‰ in a temperate saltmarsh (Eley et al., 2014). Wide variability in ε_{app} among plants presents a challenge to the accuracy of ε_{app} estimates applied to sedimentary δD_{wax}.

The seasonal timing and duration of leaf wax synthesis is also important for interpretation of δD_{wax} values. If leaf waxes are produced during discrete time intervals, δD_{wax} records in sediments may be biased toward those specific portions of the growing season. Recent evidence indicates that *n*-alkane production and δD values are an average of the growing season for temperate deciduous forests (Sachse et al., 2006, 2009; Newberry et al., 2015), but biased toward early spring leaf emergence for field grown barley (Sachse et al., 2010) and for higher elevation riparian trees (Tipple et al., 2013).

Further, while both *n*-alkanes and *n*-alkanoic acids are commonly used for leaf wax paleohydrology, relatively few calibration studies of δD_{wax} in modern vegetation have included *n*-alkanoic acids (Chikaraishi and Naraoka, 2007; Hou et al., 2007; Gao et al., 2014; Feakins et al., 2016). Therefore, the implications of using either compound for δD_p reconstructions remain largely unknown. Several surveys of vegetation and sediments suggest that leaf wax inputs from trees, especially angiosperm trees, dominate the sedimentary record over other growth forms (Sachse et al., 2006; Seki et al., 2010; Sachse et al., 2012; Tipple and Pagani, 2013; Schwab et al., 2015). Therefore this study is focused on deciduous angiosperm trees as the primary source of leaf wax to sediments. We investigated differences in the timing and amount of *n*-alkane and *n*-alkanoic acid production and seasonal changes in leaf wax and source water δD composition among five deciduous angiosperm tree species in a temperate forest. Our central objective was to better understand the controls on the δD_{wax} signal produced in species within the tree growth form and thereby improve the accuracy of ε_{app} estimates from temperate forests.

2. MATERIALS AND METHODS

2.1. Site description and environmental waters

All sample collection took place at Brown's Lake Bog State Nature Preserve (BLB; 40.6818°N, 82.0645°W; 291 masl; 0.4 km^2) in northern Ohio, USA. The biome type for BLB is a temperate deciduous broadleaf forest (Kaplan et al., 2002), and the five tree species that grow on the preserve (with mean diameter at breast height (DBH) of sampled individuals) are *Prunus serotina* (42 cm), *Acer saccharinum* (82 cm), *Quercus rubra* (144 cm), *Quercus alba* (99 cm), and *Ulmus americana* (34 cm). The site has a mean annual temperature of 10.1 °C and mean annual precipitation of 998 mm (PRISM). During the study period (March to October 2014) the mean temperature, relative humidity and total precipitation recorded at an Ohio Agricultural Research and Development Center (OARDC) weather station 15 km from BLB were 16.9 ± 6.4 °C, 78 ± 9%, and 583 mm, respectively. Additionally, a weather station (Davis Instruments, Hayward, CA, USA) was installed to log meteorological data on-site. Precipitation was sampled during each site visit from collection bottles fitted with a funnel and a layer of mineral oil to minimize evaporation. Surface waters including ephemeral pools in the forested lowlands as well as bog and lake water were also sampled during each site visit for isotope analysis.

2.2. Plant sampling

Plant material was collected over 12 visits to BLB at 1–5 week intervals from March to October 2014, with higher frequency during spring leaf emergence and expansion. Samples are referenced with the day of year (DOY) of collection (corresponding dates in Table 1 and Electronic Annex Table EA-1). When sampling took place over two consecutive days (e.g., DOY 152-153), we reference all data using the first day of collection (e.g., DOY 152). Each round of sampling included the same 2–3 individuals from each of the 5 species (11 individuals total). We analyzed a subset of one particular individual from each species ($n = 5$) over the entire time series, in addition to all individuals ($n = 11$) sampled on DOY 110, 128, 152, 235, and 274. Except where otherwise indicated, the data presented refer to the subset of 5 individuals analyzed over the entire time series.

Sampling occurred continuously over two consecutive days from approximately 9:00 am to dusk. Due to the number of trees and time-intensive sample collection from the uppermost canopy (>15 m), repeated sampling through the diel cycle to capture δD_{lw} variability was not feasible (see Section 3.4). During each sampling round, one slender branch was removed from the uppermost canopy of each individual using an arborist's slingshot. We collected sun-exposed canopy material in order to minimize potential canopy effects in leaf water or lipid isotope composition (Graham et al., 2014). Collection of plant material for molecular and isotope analysis followed the methods of Feakins and Sessions (2010) and Kahmen et al. (2013a).

Table 1
Mean fractionation of all individuals analyzed for n-C_{29} alkane and n-C_{28} alkanoic acid by DOY (top, summer buds excluded) and phenologic stage (bottom).

		$\varepsilon_{n\text{-C29/xw}}$ (‰)[a]		$\varepsilon_{n\text{-C29/MAP}}$ (‰)[b]		$\varepsilon_{n\text{-C29/lw}}$ (‰)[c]		$\varepsilon_{n\text{-C28/xw}}$ (‰)[a]		$\varepsilon_{n\text{-C28/MAP}}$ (‰)[b]		$\varepsilon_{n\text{-C28/lw}}$ (‰)[c]	
Date	DOY	Mean (1σ)	n	Mean (1σ)	n	Mean (1σ)	n	Mean (1σ)	n	Mean (1σ)	n	Mean (1σ)	n
3/23/14	82		–	−142.7 (6)	4	−136.5 (4)	2		–	−142.9 (8)	3	−134.3 (4)	2
3/30/14	89		–	−141.1 (6)	4	−137.3 (8)	4		–	−138.8 (7)	4	−135.0 (8)	4
4/5/14	95	−128.7 (7)	4	−128.2 (3)	4	−133.7 (10)	4	−127.7 (2)	2	−131.3 (15)	2	−143.9 (17)	2
4/20/14	110	−131.7 (19)	9	−119.3 (16)	9	−162.5 (10)	9	−135.5 (27)	6	−123.6 (25)	6	−167.6 (20)	6
4/27/14	117	−102.1 (25)	5	−96.9 (16)	5	−129.7 (16)	5	−112.5 (32)	2	−120.5 (14)	2	−154.5 (9)	2
5/8/14	128	−94.5 (16)	10	−95.6 (10)	9	−145.7 (16)	10	−85.3 (18)	4	−79.2 (17)	4	−133.9 (18)	5
5/19/14	139	−100.3 (10)	4	−95.7 (12)	4	−134.4 (13)	4	−86.3 (20)	3	−83.5 (16)	3	−119.5 (22)	3
6/1/14	152	−104.0 (10)	10	−101.3 (9)	11	−140.6 (10)	11	−96.6 (9)	9	−93.0 (7)	10	−131.7 (7)	10
6/26/14	177	−108.4 (8)	4	−104.8 (8)	4	−125.6 (10)[d]	4	−92.1 (4)	3	−89.4 (1)	3	−109.2 (8)	3
7/25/14	206	−108.2 (5)	2	−109.6 (10)	2	−145.6 (––)[d]	1	−92.4 (5)	2	−93.8 (1)	2	−123.8 (––)	1
8/23/14	235	−107.9 (7)	11	−107.1 (6)	11	−125.2 (10) [d]	11	−87.8 (11)	10	−87.2 (9)	10	−105.8 (12)	10
10/1/14	274	−107.2 (9)	8	−109.6 (4)	9	−126.0 (17)[d]	9	−87.9 (12)	8	−88.4 (10)	9	−105.3 (17)	9
Late bud		−132.3 (12)	14	−129.2 (15)	22	−145.9 (18)	20	−139.8 (12)	8	−136.0 (10)	15	−151.9 (21)	14
Young leaf		−94.7 (14)	18	−94.5 (10)	17	−141.4 (16)	18	−86.1 (15)	9	−84.0 (17)	9	−131.2 (18)	10
Mature leaf		−106.7 (8)	35	−105.9 (8)	37	−130.7 (14)[d]	*36*	−90.4 (11)	33	−89.8 (8)	34	−114.4 (16)	33
Summer bud		−135.6 (11)	4	−144.1 (4)	4	−141.1 (19)	4	−133.7 (12)	4	−142.3 (5)	4	−139.3 (16)	4

[a] ε_{app} based on measured δD_{xw}.
[b] ε_{app} based on modeled δD_{MAP}.
[c] ε_{bio} estimated using measured δD_{lw}.
[d] ε_{bio} estimates for the period when n-alkane synthesis ceased (DOY 177–274) are shown for completeness but note ε_{bio} values are only relevant for periods when wax synthesis is taking place.

Between 5 and 12 randomly selected leaves were stripped from the collected branch and merged into a single bulk sample per individual. Leaves (with mid-vein and petiole removed) and the branch (<1.0 cm diameter, with outer bark removed) from which leaves were stripped were immediately sealed in separate pre-ashed glass exetainer vials with airtight septa screwcaps. All samples were kept in a cooler in the field and frozen (−20 °C) in the lab until water extraction. From leaf emergence until DOY 206, an additional set of leaf samples was collected to determine leaf dry mass per area (LMA) following Cornelissen et al. (2003). Within 48 h of collection, 10 intact leaves from each individual were scanned to determine leaf area using ImageJ software (http://imagej.nih.gov/ij). The same leaves were then freeze-dried and the dry mass and area of each leaf were pooled to determine the mean LMA for each individual and sampling date.

2.3. Leaf and xylem water extraction and hydrogen isotope analysis

Leaf and xylem waters were extracted using cryogenic vacuum distillation following the methods of West et al. (2006). Exetainer vials containing frozen leaves and stems were evacuated to a pressure < 8 Pa (<60 mTorr), isolated from the vacuum pump, and heated to 100 °C. Water vapor was collected in borosilicate test tubes immersed in liquid nitrogen for a minimum of 60 min, with mean extraction times of 73 min for xylem and 63 min for leaves. To verify extraction completion, samples were weighed following cryogenic vacuum distillation and then again after freeze drying. Based on the mass difference, the recovery of plant water was >99%. Collected water was thawed and pipetted into 2 ml crimp-top vials and refrigerated at 4 °C until analysis.

Analysis of leaf and xylem water δD was made by headspace equilibration using 200 µl of water transferred to exetainer vials with a Pt catalyst added. Samples were purged using 2% H_2 in He for 10 min at 120 ml/min and equilibrated at 25 °C for at least 1 h. The isotopic composition of equilibrated headspace gas was analyzed on a Thermo Delta V Advantage isotope ratio mass spectrometer (IRMS) with a Thermo Gasbench II connected via a Conflo IV interface. Data were normalized to the V-SMOW/SLAP scale using three in-house reference standards. Precision and accuracy based on an independent standard were 1.85‰ (1σ, $n = 43$) and 0.39‰ ($n = 43$), respectively.

2.4. Lipid extraction

After extraction of bud/leaf waters, dry samples were ground to a powder. Separate aliquots of the ground bud or leaf material were used for lipid extraction and bulk $\delta^{13}C$ analysis (see Section 2.7). For lipid extraction, ~200 mg of powdered leaves were extracted by sonicating twice with 20 ml of DCM/MeOH (2:1, v/v), centrifuging and pipetting the lipid extract into a separate vial after each round of sonication. The total lipid extract was dried under a gentle stream of nitrogen and base saponified to cleave fatty esters with 3 ml of 0.5 N KOH in MeOH/H_2O (3:1, v/v) for 2 h at 75 °C. Once cool, 2.5 ml of NaCl in water (5%, w/w) was added and acidified with 6 N HCl. The solution was extracted with hexanes/DCM (4:1, v/v), neutralized with $NaHCO_3/H_2O$ (5%, w/w), and water was removed through addition of Na_2SO_4.

Compound classes were separated using 0.5 g of aminopropyl-bonded silica gel in 6 ml solid phase extraction columns. Hydrocarbons were eluted with 4 ml of hexanes, ketones were eluted with 8 ml of hexanes/DCM (6:1, v/v), alcohols were eluted with 8 ml of DCM/acetone (9:1, v/v), and acids were eluted last with 8 ml of DCM/85% formic acid (49:1, v/v). The acid fraction was evaporated under a gentle stream of nitrogen and methylated by adding ~1.5 ml of 95:5 MeOH/12 N HCl (v/v) of known δD composition and heating at 70 °C for 12–18 h. HPLC grade water was added and fatty acid methyl esters (FAMEs) were extracted with hexanes and eluted through Na_2SO_4 to remove water.

2.5. Lipid identification and quantification

n-Alkanes and FAMEs were identified by GC–MS using an Agilent 7890A GC and Agilent 5975C quadrupole mass selective detector system and quantified using a flame ionization detector (FID). Compounds were separated on a fused silica column (Agilent J&W DB-5ms) and the oven ramped from an initial temperature of 60 °C (held 1 min) to 320 °C (held 15 min) at 6 °C/min. Compounds were identified using authentic standards, fragmentation patterns and retention times. All samples were diluted in hexanes spiked with the internal standard 1,1′-binaphthyl. Compound peak areas were normalized to those of 1,1′-binaphthyl and converted to concentration using response curves for an in-house mix of *n*-alkanes and FAMEs at concentrations ranging from 0.5 to 100 µg/ml. Quantified concentrations were normalized to the mass of dry bud or leaf material extracted. Leaf wax concentration is reported as µg wax/g dry bud or dry leaf. Average chain length (ACL) is the weighted average concentration of all the long-chain waxes, defined as

$$\mathrm{ACL}_{a-b} = \sum_{i=a}^{b} \frac{i[Ci]}{[Ci]} \quad (1)$$

where $a-b$ is the range of chain lengths and C_i is the concentration of each wax compound with i carbon atoms. $ACL_{25\text{-}35}$ is used to indicate ACL values for *n*-C_{25} to *n*-C_{35} alkanes. $ACL_{24\text{-}30}$ is used to indicate ACL values for *n*-C_{24} to *n*-C_{30} alkanoic acids.

2.6. Lipid hydrogen isotope analysis

The δD composition of *n*-alkanes and *n*-alkanoic acids was determined using GC-isotope ratio mass spectrometry (GC-IRMS). A Thermo Trace GC Ultra was coupled to an IRMS via GC Isolink with pyrolysis reactor at 1420 °C and Conflo IV interface. The GC oven program ramped from 80 °C (held 2 min) to 320 °C (held 15 min) at a rate of 8 °C/min. For FAME analysis, samples and standards were run with the backflush valve open to exclude high-abundance compounds eluting before *n*-C_{22} alkanoic acid.

The H_3^+ factor was tested daily and averaged 3.8 ppm mV^{-1} during the period of analysis. Standards of known δD composition (Mix A5, F8-3; A. Schimmelmann, Indiana University) were run every 6–8 samples. Data were normalized to the V-SMOW/SLAP scale by calibrating the H_2 reference gas hydrogen isotope composition using Mix A5 and F8-3 standard analyses (see Polissar and D'Andrea, 2014). The long term standard deviation of the isotope standards was 2.3‰ (1σ, $n = 80$). The analytical uncertainty (1-standard error of the mean, SEM) is reported along with the $\delta D_{n\text{-C29 alkane}}$ and $\delta D_{n\text{-C28 acid}}$ of each sample in Table EA-1. The mean analytical uncertainty was 4.2‰ (1 s SEM, $n = 83$) for $\delta D_{n\text{-C29 alkane}}$ samples and 3.7‰ (1 s SEM, $n = 64$) for $\delta D_{n\text{-C28 acid}}$ samples. The δD value of hydrogen added to *n*-acids during derivatization was determined by mass balance of phthalic acid of known δD composition (A. Schimmelmann, Indiana University) and derivatized methyl phthalate. Hydrogen isotopic fractionations are reported as enrichment factors (in units of per mil, ‰), using the following equation:

$$\varepsilon_{a-b} = \left[\frac{(\delta D_a + 1)}{(\delta D_b + 1)}\right] - 1 \quad (2)$$

where a is the product and b is the substrate.

2.7. Bulk carbon isotope analysis

A separate aliquot of the powdered leaves was used to determine the $\delta^{13}C$ of bulk organic carbon. Bulk $\delta^{13}C$ analysis was performed via continuous flow (He; 120 ml/min) on a Costech elemental analyzer (EA) interfaced with an IRMS via a Conflo IV. $\delta^{13}C$ values were corrected for sample size dependency and normalized to the VPDB scale using a two-point calibration with IAEA calibrated (NBS-19, L-SVEC) in-house standards (−38.26‰ and −11.35‰) following Coplen et al. (2006). Error was determined by analyzing additional independent standards with a precision of 0.02‰ (1σ, $n = 28$) and accuracy of −0.01‰ ($n = 28$). All statistical analyses were performed using JMP Pro 12.0 (SAS, Cary, NC, USA).

3. RESULTS

3.1. Hydrogen isotope composition of environmental waters at Brown's Lake Bog

Hydrogen isotope data for meteoric and environmental waters at BLB are presented in Fig. 1 and Table EA-2. The δD composition of precipitation (δD_p) sampled weekly to monthly at BLB from March to October 2014 ranged from −51.5‰ (DOY 89) to −9.4‰ (DOY 152) and had a mean of -31.9 ± 13.7‰ (1σ; $n = 16$; Fig. 1). The mean modeled δD_p from the Online Isotopes in Precipitation Calculator (OIPC; Bowen and Revenaugh, 2003; Bowen, 2015) is −42.6‰ for the study period months (March to October) and −53‰ for the entire year. Similarly, precipitation collected monthly from 1966 to 1971 at a Global Network of Isotopes in Precipitation (GNIP) station in Coshocton, OH (~50 km southwest of BLB) had a mean δD_p of −37.2‰ for the study period months and −48.9‰ annually. For calculations including the δD composition of mean annual precipitation we use the OIPC value

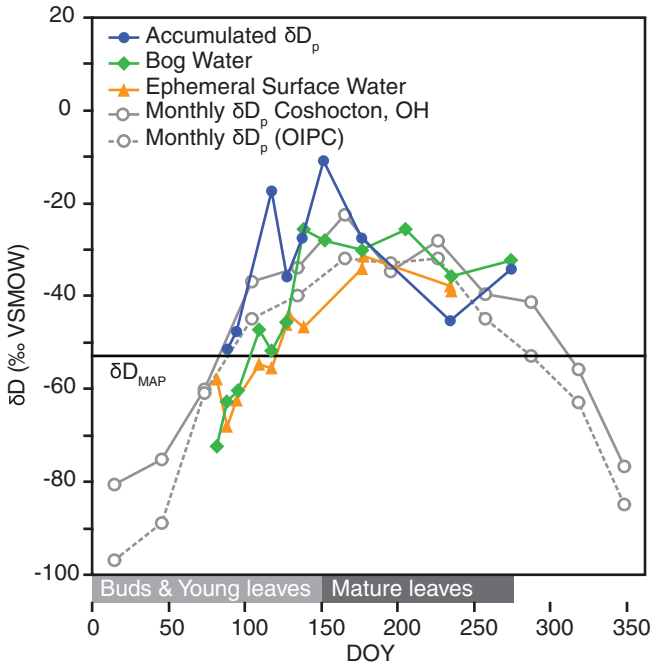

Fig. 1. Seasonal changes in environmental waters measured at BLB (closed symbols) throughout the study period (March to October). Monthly δD_p values for BLB (modeled, OIPC) and for the GNIP station in Coshocton, OH (measured, 1966–1971) are indicated with open symbols. Modeled δD_{MAP} for BLB is represented with horizontal black line. Phenologic stages prior to and during leaf maturity for trees at BLB are indicated along DOY axis.

($\delta D_{MAP} = -53‰$) because it includes the contribution of winter precipitation, which we did not sample at BLB, and because modeled δD_{MAP} values are widely used in leaf wax paleohydrology. Mean δD values for bog water and ephemeral surface waters at BLB over the study period were −43.3‰, and −47.1‰, respectively (Fig. 1).

3.2. Leaf mass per area during leaf development

Leaf area and LMA values were used to normalize wax concentration to leaf area, track the stages of leaf development, and estimate leaf photosynthetic capacity per unit area (Ellsworth and Reich, 1993; Niinemets and Tenhunen, 1997; Niinemets, 1999). All LMA data are reported in Table EA-1. The timing of leaf emergence at BLB was staggered among species by up to 18 days, which is typical for temperate sites (Maycock, 1961; Lechowicz, 1984; Wesołowski and Rowiński, 2006). LMA values in all species decreased as leaves emerged and expanded, reflecting a greater rate of increase in leaf area than leaf dry mass. Minimum LMA values, indicating full leaf expansion, were observed on DOY 139 for early-leafing species (*P. serotina*, *A. saccharinum*, and *U. americana*) and DOY 152 for late-leafing species (*Q. rubra* and *Q. alba*). The duration of leaf expansion (from leaf emergence to minimum LMA) was approximately 11 days for *U. americana*, 22–24 days for *A. saccharinum*, *Q. rubra* and *Q. alba*, and 29 days for *P. serotina*. LMA minima were followed in all species by rapid increases in LMA, reflecting mass accumulation on leaves of constant area. Mean LMA values in mature leaves were lower for *U. americana* (48.1 g/m^2) than for all other species, which ranged from 64.5 to 69.5 g/m^2. These are similar to reported values for other deciduous angiosperms (e.g., Ellsworth and Reich, 1993; Niinemets and Tenhunen, 1997; Poorter et al., 2009).

3.3. Seasonal changes in leaf wax concentration and composition

3.3.1. *n*-alkane abundance and chain length distribution

Adopting terminology from Piasentier et al. (2000), we identified three phenologic stages of leaf wax development (indicated on Fig. 2):

(i) Late bud, from first collection of buds until leaf emergence.
(ii) Young leaf, from leaf emergence until full leaf expansion (indicated by minimum LMA).
(iii) Mature leaf, from full expansion until final sample collection.

In addition, we refer to new buds produced during the summer of 2014 as summer buds.

n-Alkane concentration and ACL data are reported in Table EA-1 and Fig. 2a. Total *n*-alkane concentrations (odd chain lengths from *n*-C_{25} to *n*-C_{35}) varied widely among species and phenologic stages. Total, *n*-C_{29} and *n*-C_{31} alkane concentrations generally decreased during the bud to leaf transition before increasing at the onset of leaf maturation (DOY 152) and either stabilizing or decreasing thereafter. During the late bud stage, mean total *n*-alkane concentrations ranged among species from 35 and 57 μg/g dry bud (*Q. rubra* and *Q. alba*, respectively) to 1053 and 1822 μg/g dry bud (*P. serotina* and *A. saccharinum*, respectively). *U. americana* buds sampled on DOY 110 had a total *n*-alkane concentration of 420 μg/g dry bud. Combined, *n*-C_{29} and *n*-C_{31} alkane comprised between 42% (*A. saccharinum*) and 90% (*P. serotina* and *U. americana*) of total *n*-alkane concentrations in late buds (Fig. 2a).

During the young leaf stage, patterns of total, *n*-C_{29} and *n*-C_{31} alkane concentration changes were unique in each species. With the exception of the *Quercus* species, *n*-alkane concentrations decreased rapidly at leaf emergence (Fig. 2a). The lowest leaf *n*-alkane concentrations were observed during the young leaf stage and were followed by increases at the onset of the mature leaf stage (DOY 152-274) in all species except *U. americana* (Fig. 2a). The largest increases in total *n*-alkane concentration from leaf emergence to full expansion (DOY 152) were observed in *Q. rubra* and *P. serotina* (15- and 7-fold increases, respectively). Following full leaf expansion, *n*-alkane concentrations stabilized in *A. saccharinum* and gradually decreased by 26–63% through the summer and fall (DOY 152-274) in all other species. Mean total *n*-alkane concentrations in mature leaves ranged among species by an order of magnitude, from 132 μg/g in *U. americana*, 166 μg/g in *Q. alba*, and 578 μg/g in *A. saccharinum*, to 1968 μg/g in *Q. rubra* and 2586 μg/g in *P. serotina*. These are similar to previously reported *n*-alkane concentrations in leaves of the same genera and species (Diefendorf et al., 2011). Combined, *n*-C_{29} and *n*-C_{31} alkane comprised between 72% and 98% of total *n*-alkane concentrations in mature leaves of each species except *Q. alba*, in which they comprised 40%.

In all species, $ACL_{25\text{-}35}$ values decreased during bud swell and increased during leaf expansion (Fig. 2a). $ACL_{25\text{-}35}$ values were stable in mature leaves ($1\sigma < 0.3$ in all species), consistent with a prior study that observed no significant change in ACL from summer to fall (Bush and McInerney, 2013). Mean $ACL_{25\text{-}35}$ values for mature leaves (DOY 152-274) were 27.5 for *Q. alba*, 29.1 for *U. americana*, 29.2 for *A. saccharinum*, 29.7 for *Q. rubra*, and 31.0 for *P. serotina*.

3.3.2. *n*-alkanoic acid abundance and chain length distribution

n-Alkanoic acid concentration and ACL data are reported in Table EA-1 and Fig. 2b. Total *n*-alkanoic acid concentrations (even chain lengths from *n*-C_{24} to *n*-C_{30}) were relatively high in late buds, decreased during leaf emergence, and increased throughout the mature leaf stage (Fig. 2b). Total *n*-alkanoic acid concentrations in the late buds of each species ranged from 114 to 279 μg/g dry bud. All species had sharp decreases in $ACL_{24\text{-}30}$ during leaf emergence and expansion, reflecting complete turnover of *n*-C_{30} alkanoic acid in all species and *n*-C_{28} alkanoic acid in most species (Fig. 2b). Total, *n*-C_{28} and *n*-C_{30} alkanoic acid concentrations increased throughout the mature leaf stage and reached their highest respective concentrations in each species at the end of the growing season (DOY 274). Mean total *n*-alkanoic acid concentrations in mature

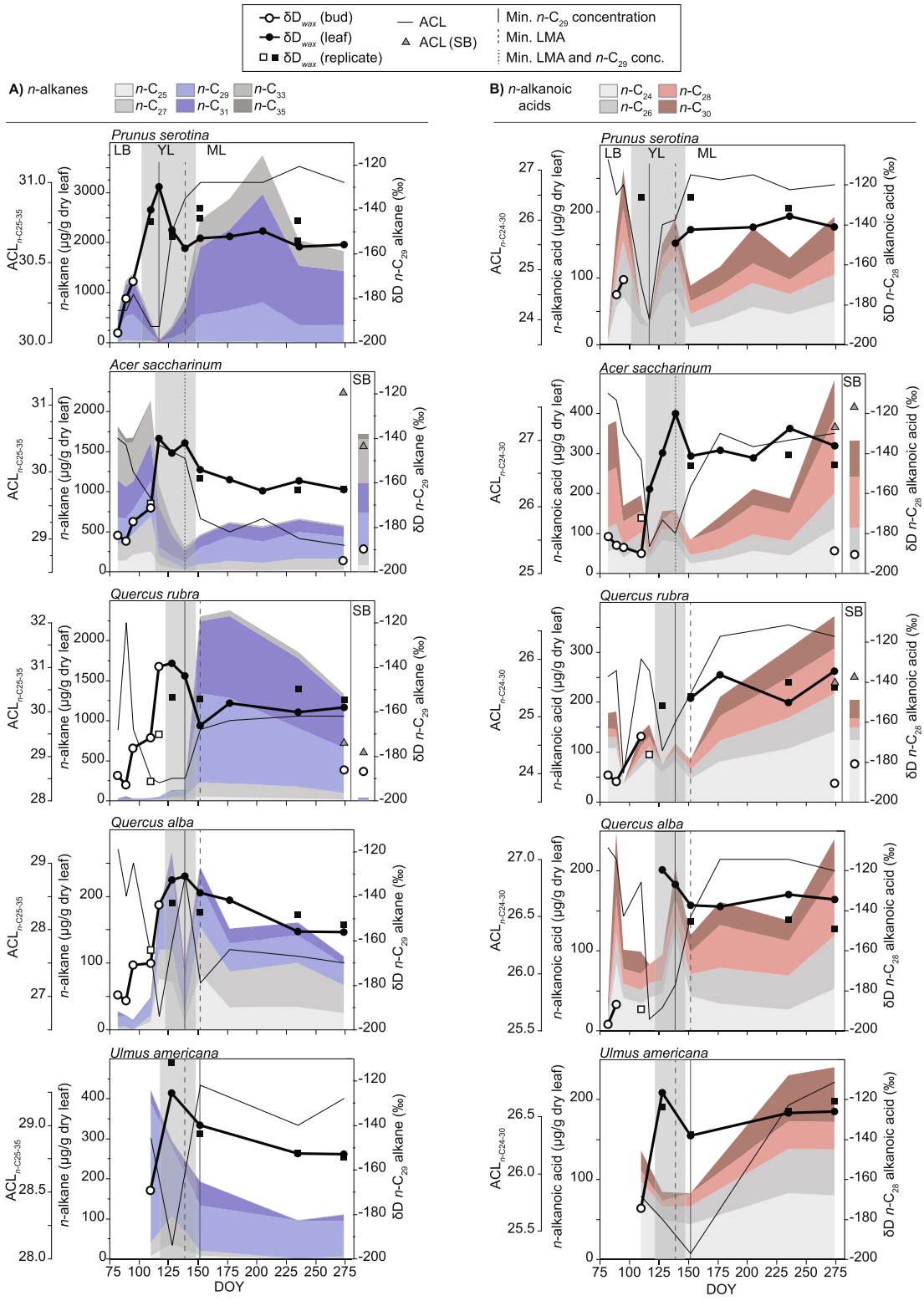

Fig. 2. Seasonal changes in lipid concentration (shaded layers), ACL (thin black line) and δD values (thick black lines and circles) for *n*-alkanes (A) and *n*-alkanoic acids (B) from a single individual from each species. Black squares show δD_{wax} values from biological replicates of each species. The stages of leaf development are initialed LB (late bud), YL (young leaf, shaded area), and ML (mature leaf). Vertical lines mark the DOY of minimum *n*-C_{29} alkane concentration (based on leaf dry mass and area, solid lines), minimum LMA (long dashes), or both (short dashes). Open symbols indicate data for buds; closed symbols indicate leaves. Summer buds are indicated with open symbols on DOY 274. Right panels labeled "SB" for *A. saccharinum* and *Q. rubra* represent lipid concentration (stacked bars), ACL (triangles) and δD data (open circles) from buds collected the following winter. Note different scales for leaf wax concentration and ACL. Analytical uncertainty for δD_{wax} measurements is 4‰.

leaves ranged among species from 141 μg/g dry leaf in *P. serotina* to 243 μg/g dry leaf in *Q. rubra*. Combined, *n*-C_{28} and *n*-C_{30} alkanoic acid comprised between 41% and 46% of total *n*-alkanoic acid concentrations in mature leaves of each species except *A. saccharinum* in which they comprised 63%. Minimum $ACL_{24\text{-}30}$ values were observed in all species during the young leaf stage due to turnover of longer chain-lengths. Thereafter, $ACL_{24\text{-}30}$ increased due to higher *n*-C_{28} and *n*-C_{30} alkanoic acid production, and stabilized between 25.9 and 27.4 in the mature leaves of all species and individuals.

There were several key differences in the abundance and distribution of *n*-alkanes and *n*-alkanoic acids. First, total *n*-alkanoic acid concentrations and interspecies variability in mature leaves (187 ± 123 μg/g dry leaf) were both lower than observed for *n*-alkanes (1077 ± 1020 μg/g dry leaf; Fig. 2). Second, while *n*-alkane concentrations in mature leaves of all species were dominated by *n*-C_{29}, and *n*-C_{31} (mean $ACL_{25\text{-}35}$ = 29.3 ± 0.2), there was a less pronounced preference for any particular *n*-alkanoic acid chain length (mean $ACL_{24\text{-}30}$ = 26.7 ± 0.6; Fig. 2). Third, loss of longer chain lengths during leaf expansion was common to both compound classes, but complete turnover during this stage was unique to *n*-alkanoic acids (see Section 4.3). Lastly, while *n*-alkane concentrations were either stable or decreased through the mature leaf stage, *n*-alkanoic acid concentrations increased in all species over the same interval.

3.4. Plant source waters: xylem and leaf water δD

Plant water δD data are reported in Table EA-1 and Fig. 3. Mean δD_{xw} for all sampled species and individuals was -50.0 ± 10‰ (1σ; $n = 70$) over the study period and −51.8 ± 6‰ (1σ, $n = 35$) during the mature leaf stage. This is similar to the OIPC modeled δD_{MAP} (−53‰), and significantly D-depleted relative to modeled δD_p (−42.6 ± 10.6‰, 1σ, *t*-test, $p = 0.048$) and measured δD_p (−31.9 ± 13.7‰, 1σ, *t*-test, $p < 0.0001$) for the same period (March-October). Mean δD_{xw} values during each stage of leaf development were not significantly different for *P. serotina*, *A. saccharinum*, or *U. americana* (one-way ANOVA, $p = 0.2$, 0.4, 0.8, respectively) but were for *Q. alba* and *Q. rubra* (one-way ANOVA, $p = 0.0004$, 0.001, respectively). Xylem water was significantly more D-enriched prior to leaf maturity in *Q. alba* and *Q. rubra* (−35‰ and −42‰, respectively) than during the mature leaf stage (−51‰ and −55‰, respectively).

Mean δD_{lw} (including both buds and leaves) for all species and individuals over the study period was −21.5 ± 21.7‰ (1σ, $n = 77$), which was significantly more positive and more variable than δD_{xw} (−50.0 ± 10‰ (1σ, $n = 70$); *t*-test, $p < 0.0001$). The fractionation between δD_{lw} and δD_{xw} ($\varepsilon_{lw\text{-}xw}$) was significantly higher during the young leaf stage (55.1‰) than either the late bud (20.8‰) or mature leaf (28.2‰) stages (*t*-test, $p < 0.0001$), indicating D-enrichment of leaf water during the transition from bud to leaf, and D-depletion as leaves reached full expansion and maturity (Fig. 3). The mean δD_{lw} values for the late bud, young leaf and mature leaf stages (−32.4‰,

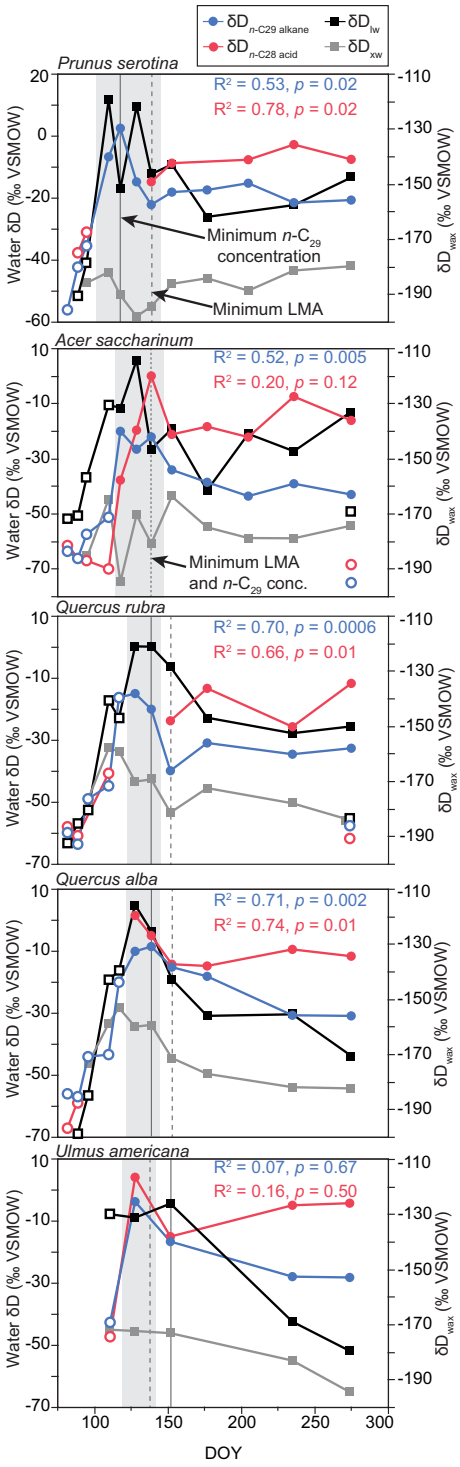

Fig. 3. Seasonal changes in the δD composition of xylem water (gray squares), leaf water (black squares), *n*-alkanes (blue circles) and *n*-alkanoic acids (red circles) in buds (open symbols) and leaves (closed symbols). Correlations of δD_{lw} with $\delta D_{n\text{-}C29\ alkane}$ and $\delta D_{n\text{-}C28\ acid}$ are given in blue and red text, respectively. The young leaf stage is indicated with gray shading. Summer buds of *A. saccharinum* and *Q. rubra* are indicated with open symbols on DOY 274. Data for a single individual from each species. (For interpretation of the references to colour in this figure legend, the reader is referred to the web version of this article.)

1.5‰, and −24.2‰, respectively) were significantly different (one-way ANOVA, $p < 0.0001$). The magnitude of leaf water D-enrichment during bud swelling and leaf emergence was 57‰ in *A. saccharinum*, 63‰ in *P. serotina* and *Q. rubra*, and 73‰ in *Q. alba* (Fig. 3). Sampling only permitted one bud water sample for *U. americana*.

Single point measurements of δD_{lw} are problematic due to observed diurnal δD_{lw} variability (Cernusak et al., 2002; Eley et al., 2014; Cernusak et al., 2015). Therefore, we applied an expanded Craig-Gordon model described by Roden et al. (2000) to estimate the diurnal range (9:00–18:00 h) of δD_{lw} using the following inputs: measured δD_{xw} for each individual and sampling date, measured atmospheric water vapor δD sampled on DOY 116, 128, 138, 152, 205, and 275 (reported in Table EA-2) using the cryogenic sampling apparatus described in Helliker et al. (2002); atmospheric pressure from a weather station installed at BLB; hourly relative humidity and temperature data from the OARDC weather station; and the mean stomatal conductance of 69 mmol m^{-2} s^{-1} measured for broadleaf angiosperm trees *Quercus prinus* and *Acer rubrum* at a temperate site in Pennsylvania in August (Song et al., 2013). Modeled δD_{lw} values were typically lowest in the morning and increased to peak values between 14:00 and 18:00 h. The diurnal range in modeled δD_{lw} varied from 2‰ to 22‰ for each individual and date. By comparison, measured δD_{lw} ranged by 10–30‰ among individuals on a given date.

3.5. Seasonal development of *n*-alkane hydrogen isotopes

3.5.1. *n*-Alkane hydrogen isotope composition

Hydrogen isotope analysis was carried out on all *n*-alkane chain lengths of adequate concentration. The following discussion focuses on the δD composition of *n*-C_{29} alkane, which is frequently used in leaf wax paleohydrology and was generally the most abundant chain length in trees sampled at BLB. The δD composition of additional chain lengths is reported in Table EA-1. The δD values of major long-chain *n*-alkane homologs (*n*-C_{27}, *n*-C_{29}, *n*-C_{31}) of all sampled individuals and species over the entire growing season were strongly correlated (*n*-C_{27} and *n*-C_{29}, $R^2 = 0.79$, $p < 0.0001$; *n*-C_{29} and *n*-C_{31}, $R^2 = 0.87$, $p < 0.0001$).

In all species, $\delta D_{n\text{-C29 alkane}}$ fluctuated between DOY 89-152 and generally stabilized thereafter. The δD composition of *n*-C_{29} alkane was most negative in late buds and most positive either at or immediately following leaf emergence (Fig. 2a). Total D-enrichment during the transition from late bud to young leaf was 66‰ for *P. serotina*, 56‰ for *Q. alba*, 55‰ for *Q. rubra*, 46‰ for *A. saccharinum*, and 44‰ for *U. americana*, comparable to prior observations of woody broadleaf angiosperms (Tipple et al., 2013; Oakes and Hren, 2016). The timing of *n*-alkane D-enrichment corresponded with the greatest bud and leaf water D-enrichment (Fig. 3). As leaves reached full expansion on DOY 152, $\delta D_{n\text{-C29 alkane}}$ values of all species became more negative, dropping by ~24–29‰ relative to peak young leaf values. After DOY 152, $\delta D_{n\text{-C29 alkane}}$ values were stable in *P. serotina*, *A. saccharinum* and *Q. rubra* and decreased by 13‰ and 18‰ in *U. americana* and *Q. alba*, respectively, before stabilizing in late summer (Fig. 2a). As mature leaves approached senescence interspecies $\delta D_{n\text{-C29 alkane}}$ variability decreased. The mean $\delta D_{n\text{-C29 alkane}}$ for all species and individuals was −154.4 ± 5.4‰ (1σ, $n = 11$) on DOY 235 and −156.7 ± 3.8‰ (1σ, $n = 9$) on DOY 274.

3.5.2. Hydrogen isotope fractionation in n-alkanes

All hydrogen isotope fractionation data are included in Table EA-1 and summarized by DOY and phenologic stage in Table 1. The net δD fractionation between the biosynthetic water pool and resulting leaf wax (ε_{bio}) is not directly measurable. However, the biosynthetic water pool is fed in large part by leaf water. Therefore, prior studies have approximated ε_{bio} values using δD_{wax} and measured or modeled δD_{lw} (Kahmen et al., 2013a,b; Newberry et al., 2015; Sachse et al., 2015). We approximate ε_{bio} for *n*-C_{29} alkane ($\varepsilon_{n\text{-C29/lw}}$) based on measured $\delta D_{n\text{-C29 alkane}}$ and measured δD_{lw}. Because ε_{bio} is a measure of δD fractionation during wax synthesis, we restrict ε_{bio} estimates to portions of the growing season when *n*-alkanes are being produced (approximately from leaf emergence to full expansion). Mean $\varepsilon_{n\text{-C29/lw}}$ estimates for this period were −147‰ for *Q. rubra* and *P. serotina* (±11‰ and 14‰, 1σ, respectively), −138 ± 14‰ (1σ) for *A. saccharinum*, −135 ± 11‰ (1σ) for *Q. alba*, and −129 ± 10‰ (1σ) for *U. americana*.

Values of apparent fractionation based on $\delta D_{n\text{-C29 alkane}}$ and either δD_{xw} ($\varepsilon_{n\text{-C29/xw}}$) or the δD of modeled mean annual precipitation ($\varepsilon_{n\text{-C29/MAP}}$) were in close agreement throughout the growing season (Table 1). Mean $\varepsilon_{n\text{-C29/xw}}$ values were significantly different during the late bud, young leaf and mature leaf stages (one-way ANOVA, $p < 0.0001$), and interspecies variability decreased through the late summer and autumn. Mean $\varepsilon_{n\text{-C29/MAP}}$ values for all species and individuals prior to senescence were similar on DOY 235 (−107.1 ± 6‰, 1σ, $n = 11$) and 274 (−109.6 ± 4‰, 1σ, $n = 9$). For comparison, the mean $\varepsilon_{n\text{-C29/MAP}}$ for all previously published dicot trees sampled in temperate sites from August to November (when we expect δD_{wax} values are stable and *n*-alkane synthesis has ceased), is −121.2 ± 14.9‰ (1σ, $n = 67$) (Sachse et al., 2006; Hou et al., 2007; Sachse et al., 2009; Tipple and Pagani, 2013).

3.6. Seasonal development of n-alkanoic acid hydrogen isotopes

3.6.1. *n*-Alkanoic acid hydrogen isotope composition

Hydrogen isotope analysis was carried out on all long-chain *n*-alkanoic acid homologs (*n*-C_{26}, *n*-C_{28}, *n*-C_{30}) where concentration permitted. Our discussion is focused on *n*-C_{28} alkanoic acid and δD values for additional *n*-alkanoic acid chain lengths are reported in Table EA-1. The δD values of long-chain *n*-alkanoic acid homologs (*n*-C_{26}, *n*-C_{28}, *n*-C_{30}) of all sampled individuals and species over the entire growing season were strongly correlated (*n*-C_{26} and *n*-C_{28}, $R^2 = 0.73$, $p < 0.0001$; *n*-C_{30} and *n*-C_{28}, $R^2 = 0.88$, $p < 0.0001$).

The magnitude of D-enrichment in $\delta D_{n\text{-C28 acid}}$ during the transition from late buds to young leaves was 70‰ for *A. saccharinum*, 67‰ for *Q. alba* and 57‰ for *U. americana*. This is 11–24‰ greater than observed for $\delta D_{n\text{-C29 alkane}}$ in the same

individuals. Due to complete turnover of n-C_{28} alkanoic acid during the young leaf stage, $\delta D_{n\text{-C28 acid}}$ data were sparse for the young leaves of *P. serotina* and *Q. rubra*, in which the D-enrichment was 18‰ and 19‰, respectively (48‰ and 36‰ less than observed for $\delta D_{n\text{-C29 alkane}}$ in the same individuals). $\delta D_{n\text{-C28 acid}}$ values fluctuated prior to full leaf expansion and stabilized thereafter in all species except *U. americana*, for which $\delta D_{n\text{-C28 acid}}$ increased by 12‰ throughout the mature leaf stage (Fig. 2b). Overall, $\delta D_{n\text{-C28 acid}}$ values in mature leaves (-138.0 ± 7.5‰, 1σ, $n = 34$) were significantly more positive than in late buds (-182 ± 9‰, 1σ, $n = 15$; t-test, $p < 0.0001$). Prior to leaf shed (DOY 274) mean $\delta D_{n\text{-C28 acid}}$ among all species and individuals was -136.8 ± 9.1‰ (1σ, $n = 9$).

3.6.2. Hydrogen isotope fractionation in n-alkanoic acids

We approximate ε_{bio} for n-C_{28} alkanoic acid ($\varepsilon_{n\text{-C28/lw}}$) based on measured $\delta D_{n\text{-C28 acid}}$ and δD_{lw}. The majority of n-C_{28} alkanoic acid synthesis took place throughout the mature leaf stage following full leaf expansion. Mean $\varepsilon_{n\text{-C28/lw}}$ estimates during the mature leaf stage were -119‰ for *Q. rubra* and *P. serotina* (± 14‰ and 15‰, 1σ, respectively), -114‰ for *A. saccharinum* and *Q. alba* ($\pm$ 16‰ and 13‰, 1σ, respectively), and -106 ± 23‰ (1σ) for *U. americana*. $\varepsilon_{n\text{-C28/lw}}$ estimates were 21–28‰ more positive than $\varepsilon_{n\text{-C29/lw}}$ in the same species (Table 1).

Values of apparent fractionation based on $\delta D_{n\text{-C28 acid}}$ and either δD_{xw} ($\varepsilon_{n\text{-C28/xw}}$) or modeled δD_{MAP} ($\varepsilon_{n\text{-C28/MAP}}$) were in close agreement throughout the growing season (Table 1). Mean $\varepsilon_{n\text{-C28/xw}}$ values during the late bud stage (-139.8 ± 12.2‰, 1σ, $n = 8$) were significantly more negative than the mature leaf stage (-90.4 ± 10.5‰, 1σ, $n = 33$; t-test, $p < 0.0001$). Toward the end of the growing season, mean $\varepsilon_{n\text{-C28/MAP}}$ was constant from DOY 235 to 274 (-88‰) although the interspecies variability (9.6‰, 1σ) was more than twice that of $\varepsilon_{n\text{-C29/MAP}}$ (4.1‰, 1σ). Mean $\varepsilon_{n\text{-C28/MAP}}$ on DOY 274 was 21‰ more positive than mean $\varepsilon_{n\text{-C29/MAP}}$.

3.7. Bulk foliar $\delta^{13}C$ values

Bulk foliar $\delta^{13}C$ values generally decreased from young leaves to mature leaves (Fig. 4), as observed in prior studies (Cernusak et al., 2009; McKown et al., 2013; Newberry et al., 2015). Mean bulk $\delta^{13}C$ was -27.1‰ for late buds, -26.6‰ for young leaves, and -28.1‰ for mature leaves. Bulk $\delta^{13}C$ increased during the transition from late buds to young leaves, and became increasingly negative as leaves matured through the summer and autumn. On DOY 274 the bulk $\delta^{13}C$ of summer buds was identical to that of mature leaves from the same individual (Fig. 4). The total growing season range in bulk $\delta^{13}C$ was lowest in *P. serotina* (2.6‰) and highest in *Q. alba* (4.1‰).

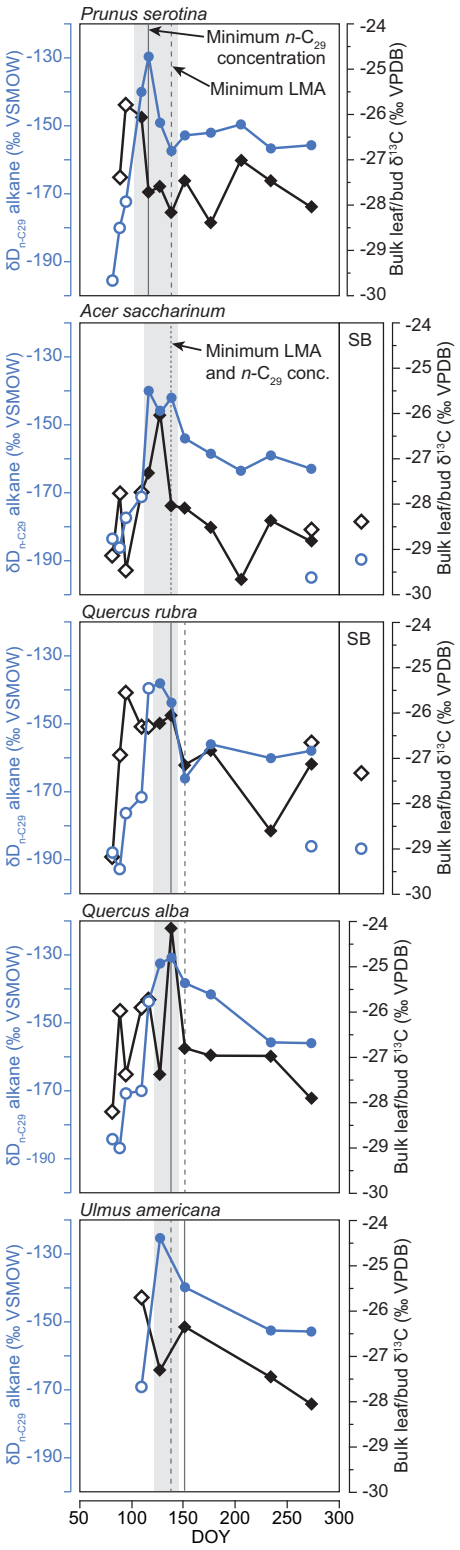

Fig. 4. Seasonal changes in $\delta D_{n\text{-C29 alkane}}$ (blue circles) and bulk foliar $\delta^{13}C$ (black diamonds) observed in buds (open symbols) and leaves (closed symbols) of one individual from each species. Summer buds sampled the following winter from *A. saccharinum* and *Q. rubra* are in panels labeled SB. The young leaf stage is indicated with gray shading. (For interpretation of the references to colour in this figure legend, the reader is referred to the web version of this article.)

4. DISCUSSION

4.1. Timing of *n*-alkane synthesis

Leaf wax concentration reflects net wax production and removal through mechanical stresses including ablation via

wind and rain (Shepherd and Griffiths, 2006). At times when rates of removal exceed production, leaf wax concentration will decrease despite continued synthesis. Therefore, we use the additional indicators of ACL (indicating production or loss of different chain lengths) and δD_{wax} (reflecting wax synthesis using H with different δD values) to constrain the timing of *de novo* leaf wax synthesis.

In all tree species at BLB, *n*-alkane production occurred at variable rates from the first collection of late buds through the onset of leaf maturity (DOY 152), and ceased thereafter, as indicated by stable or decreasing concentrations through the summer. This seasonal pattern is common in deciduous angiosperm trees and shrubs (Jetter and Schaeffer, 2001; Sachse et al., 2009; Tipple et al., 2013; Newberry et al., 2015; Oakes and Hren, 2016). By contrast, *n*-alkane production may continue through the summer and autumn in mature leaves of evergreen gymnosperms and angiosperms (Sachse et al., 2015; Oakes and Hren, 2016). At BLB, total *n*-alkane concentrations generally increased in swelling buds (by 20–600%) while $\delta D_{n\text{-C29 alkane}}$ values increased (Fig. 2a). Late bud $\delta D_{n\text{-C29 alkane}}$ increases began 18–39 days prior to leaf emergence, indicating *de novo* *n*-alkane synthesis (using an increasingly D-enriched H source) as buds swell. Simultaneous decreases in $ACL_{25\text{-}35}$ indicate that synthesis in buds is dominated by *n*-C_{25} through *n*-C_{29} alkane, while longer chain lengths are lost.

Leaf area expansion (decreasing LMA) during the young leaf stage coincided with decreasing *n*-alkane concentrations in most species (Fig. 2a). Leaf wax concentrations are typically determined based on the mass of dry leaf extracted. However, because waxes accumulate in layers over leaf surfaces, either embedded within the cuticle or as an epicuticular film (Eglinton and Hamilton, 1967; Jetter et al., 2006), dispersal of a fixed amount of wax over an increasing leaf surface could result in an apparent drop in *n*-alkane concentrations during leaf expansion. Converting from mass-based to leaf area-based *n*-alkane concentration using LMA (e.g., Wright et al., 2004) revealed a significant positive correlation between the two measures of *n*-alkane abundance (μg *n*-C_{29}/cm^2 and μg *n*-C_{29}/g dry leaf extracted, $R^2 = 0.90$, $p < 0.0001$). Therefore, rapidly decreasing *n*-alkane concentrations in the young leaf stage following leaf emergence (e.g., *P. serotina*, *A. saccharinum*, *Q. alba*) may be due to dilution of pre-existing bud *n*-alkanes over an increasing leaf area. Baker and Hunt (1981) suggested that apparent decreases in wax concentrations in *Prunus* following bud break reflect rapid leaf expansion. Despite apparent loss over this period, bud *n*-alkanes can be retained and contribute to the wax composition of the forming leaf. However in certain species (e.g., *Q. rubra*, *P. serotina*) this contribution is likely swamped by relatively large amounts of *n*-alkanes produced *de novo* during leaf development.

We mark the beginning of *de novo* *n*-C_{29} alkane accumulation in leaves at the date of minimum *n*-C_{29} alkane concentrations (determined by leaf mass and area), between 7 and 24 days after leaf emergence (indicated with dotted vertical lines in Figs. 2–4). Rapid increases in *n*-alkane concentrations (total and *n*-C_{29}) at the onset of the mature leaf stage (Fig. 2a) suggest an increased rate of *n*-alkane production as leaves reach full expansion. Similarly, Hauke and Schreiber (1998) found that major *n*-alkane production did not take place until 23–28 days after leaf emergence in *Hedera helix* (ivy) leaves.

Changes in *n*-alkane production and composition over the first 9 weeks of the BLB growing season may be linked to shifting plant metabolism during the early stages of leaf development. Young leaves are heterotrophic and depend on stored carbohydrate reserves for synthesis of new compounds. By contrast, mature leaves are autotrophic and generally rely on photosynthesis (Turgeon, 1989; Cernusak et al., 2009; Pantin et al., 2011). In dicotyledonous plants, the metabolic transition from heterotroph to autotroph takes place when the leaf is 30–60% fully expanded (Turgeon, 1989). As the lamina expands, rates of photosynthesis increase while rates of respiration decrease (Collier and Thibodeau, 1995; Pantin et al., 2011). For all tree species at BLB, maximum leaf area was observed 24–35 days after leaf emergence. Therefore, we estimate that the metabolic transition occurs ~12–17 days after leaf emergence (equivalent to 30–60% of full expansion). This timing corresponds both with peak $\delta D_{n\text{-C29 alkane}}$ values and minimum *n*-C_{29} alkane concentrations (Fig. 2a, dotted vertical lines). Therefore, we suggest that leaves are net heterotrophs prior to the date of minimum *n*-C_{29} alkane concentration, and have developed sufficient photosynthetic capacity to operate as net autotrophs after this point. This is supported by bulk leaf $\delta^{13}C$ data (Fig. 4), with young leaves significantly ^{13}C-enriched relative to mature leaves (−26.6‰ and −28.1‰, respectively; *t*-test, $p < 0.0001$). Prior studies have established that heterotrophic developing leaves are ^{13}C-enriched relative to autotrophic mature leaves (Leavitt and Long, 1985; Damesin et al., 1998; Damesin and Lelarge, 2003; Cernusak et al., 2009). All tree species at BLB had peak $\delta^{13}C$ values just prior to full leaf expansion (minimum LMA) and decreasing $\delta^{13}C$ values thereafter (Fig. 4), indicating a metabolic shift just prior to leaf maturity. Phenologic regulation of leaf wax synthesis based on shifts from heterotrophic to autotrophic growth appears to be a critical control on the timing of leaf wax synthesis as well as the partitioning of hydrogen sources (see Section 4.2).

Results from BLB suggest that *n*-alkane production ceases in mature leaves, indicated by relatively constant ACL and $\delta D_{n\text{-C29 alkane}}$ and stable or decreasing *n*-alkane concentrations during the mature leaf stage. Total *n*-alkane concentrations in autumn were 26–63% lower than at full leaf expansion (for all species except *A. saccharinum*), perhaps due to ablation from the leaf surface (Jetter and Schaeffer, 2001). If the observed loss of *n*-alkanes from mature summer leaves is due to ablation, this could contribute to a regionally integrated *n*-alkane component in atmospheric dust or aerosols.

Summer buds sampled on DOY 274 and during the following winter from *A. saccharinum* and *Q. rubra* had total *n*-alkane concentrations, ACL and $\delta D_{n\text{-C29 alkane}}$ values that were distinct from those in co-occurring mature leaves and instead were similar to those observed in the late buds of the same individuals (Fig. 2a). This indicates that major production of late bud *n*-alkanes takes place during sum-

mer bud set and that these compounds are retained over the winter, establishing set points for leaf wax abundance and δD values in the late buds of the following growing season, as suggested previously (Tipple et al., 2013).

4.2. Controls on δD of n-C_{29} alkane

One objective of this study was to determine when $\delta D_{n\text{-C29 alkane}}$ values of leaves are established and the factors controlling $\delta D_{n\text{-C29 alkane}}$ as leaves develop. At BLB, $\delta D_{n\text{-C29 alkane}}$ values were lowest in late buds ($-175 \pm 14‰$, 1σ, $n = 22$), highest in young leaves ($-140 \pm 11‰$, 1σ, $n = 18$), and became relatively D-depleted in mature leaves ($-153 \pm 7‰$, 1σ, $n = 37$). The possible drivers of distinct $\delta D_{n\text{-C29 alkane}}$ values among the phases of leaf development are changes in source water δD, changes in leaf water δD, and changes in leaf metabolism. Below we demonstrate that data from BLB are consistent with the latter two factors.

Vascular plants take up precipitation-fed soil water through roots and into xylem, during which there is no isotopic fractionation (Dawson and Ehleringer, 1993; Dawson et al., 2002). Therefore, δD_{xw} values directly reflect plant source water δD. At BLB mean δD_{xw} across the stages of leaf development was invariable for all species except *Q. alba* and *Q. rubra*, which had 10–17‰ higher δD_{xw} during leaf emergence and expansion than during the mature leaf stage. Similar patterns have been observed in both arid and humid coastal sites in the western US (Phillips and Ehleringer, 1995; Tipple et al., 2013; Sachse et al., 2015). Higher δD_{xw} values during leaf formation may be due to retention of D-enriched winter sap (Phillips and Ehleringer, 1995; Tipple et al., 2013), and may be specific to late-leafing species (e.g., *Q. rubra* and *Q. alba* at BLB). Staggered bud break among species is controlled by the diameter and density of xylem vessels in earlywood (Lechowicz, 1984). Late-leafing species undergo xylem cavitation in winter and regeneration during leaf expansion (Turgeon, 1989). This process may cause evaporative D-enrichment of xylem water in late-leafing species and thus may contribute to D-enrichment of leaf wax prior to leaf maturity. While elevated δD_{xw} was observed in late-leafing *Q. alba* and *Q. rubra*, the magnitude (10–17‰) was insufficient to account for $\delta D_{n\text{-C29 alkane}}$ increases of 44–66‰ over the same interval. Based on this evidence, source water δD may have a small influence on $\delta D_{n\text{-C29 alkane}}$ values in late-leafing species, but has no direct influence on other species, consistent with prior observations (Tipple et al., 2013; Newberry et al., 2015; Oakes and Hren, 2016).

The magnitude of D-enrichment in $\delta D_{n\text{-C29 alkane}}$ during the transition from late bud to young leaf (44–66‰ among species) was consistent with that observed in bud and leaf water over the same period (Fig. 3; 57–73‰). We suspect this rapid increase in δD_{lw} may reflect intensified transpirational D-enrichment in swelling buds and expanding leaves prior to development of the cuticle, which limits water loss (Riederer and Schreiber, 2001). Leaf transpiration rates typically increase during leaf emergence and peak as leaves reach 25–100% of the final leaf area (Constable and Rawson, 1980; Hauke and Schreiber, 1998; Pantin et al., 2012). Indeed, δD_{lw} values at BLB peaked prior to full leaf expansion (DOY 152) (Fig. 3, dotted lines). As leaves reached full expansion and n-alkane production intensified, we observed simultaneous D-depletion in $\delta D_{n\text{-C29 alkane}}$ and δD_{lw} of 19–27‰ and 23–36‰, respectively, perhaps reflecting sufficient cuticular development to prevent further transpirational leaf water D-enrichment (Fig. 3). For the entire growing season, all species except *U. americana* had a significant positive correlation between δD_{lw} and $\delta D_{n\text{-C29 alkane}}$ (Fig. 3; *P. serotina* $R^2 = 0.53$, $p = 0.02$; *A. saccharinum* $R^2 = 0.52$, $p = 0.005$; *Q. rubra* $R^2 = 0.70$, $p = 0.0006$; *Q. alba* $R^2 = 0.71$, $p = 0.002$). When regressions are limited to the main period of *de novo* n-alkane synthesis (DOY 82-152), R^2 values increase slightly, ranging from 0.56 to 0.78. This suggests that δD_{lw} is the primary control on $\delta D_{n\text{-C29 alkane}}$, as previously found for dicotyledonous angiosperms in controlled growth experiments and in natural settings (Kahmen et al., 2013a,b; Tipple et al., 2015).

A secondary driver of $\delta D_{n\text{-C29 alkane}}$ variability may be metabolic shifts as leaves develop, as suggested previously (Schmidt et al., 2003; Sessions, 2006; Newberry et al., 2015; Sachse et al., 2015). Heterotrophic plant tissues have more positive δD_{wax} values than autotrophic tissues because the former source hydrogen from relatively D-enriched NADPH derived from stored carbohydrates rather than from cellular water as during photosynthesis (Sessions, 2006; Gamarra and Kahmen, 2015). At BLB, $\delta D_{n\text{-C29 alkane}}$ values increased throughout the late bud stage, signaling that *de novo* n-alkane production prior to the metabolic transition may rely in part on D-enriched NADPH derived from stored reserves. The timing of peak $\delta D_{n\text{-C29 alkane}}$ values coincides with the estimated metabolic transition based on peak bulk leaf $\delta^{13}C$ values (Fig. 4). Subsequently, $\delta D_{n\text{-C29 alkane}}$ values decreased by 19–27‰, perhaps in part due to the transition toward net autotrophy in mature leaves and reliance on relatively D-depleted NADPH derived from cellular water. Therefore, while δD_{lw} controls up to 56–78% of changes in $\delta D_{n\text{-C29 alkane}}$ during the period of *de novo* synthesis, the transition from heterotrophic to autotrophic growth may explain the remaining variability.

4.3. Timing of n-alkanoic acid synthesis

Full loss of long-chain waxes during the young leaf stage was unique to the n-alkanoic acids and serves as direct evidence that *de novo* synthesis of these chain lengths is initiated during leaf expansion. It is possible that complete turnover of n-C_{28} and/or n-C_{30} alkanoic acids reflects conversion of n-alkanoic acid precursors to n-alkanes in developing leaves (Chikaraishi and Naraoka, 2007). Increasing concentrations through the summer and autumn indicate that n-C_{28} alkanoic acid is synthesized continuously throughout the growing season, unlike n-C_{29} alkane. Therefore, continuous n-alkanoic acid synthesis may result in a seasonally-integrated record, while discrete timing of synthesis may bias n-alkane records toward the early growing season.

n-Alkane concentrations decreased through the summer and autumn (Fig. 2a). If loss of n-alkanes were driven by

ablation of the epicuticular film from pervasive environmental conditions such as wind or rain, we would also expect loss of *n*-alkanoic acids, which we did not observe. Therefore, either *n*-alkanoic acids are more resistant to ablation than *n*-alkanes, perhaps due to their different morphology or position within the cuticle (Kunst et al., 2008), or decreasing *n*-alkane concentrations reflect conversion in the cuticle to other wax constituents (Jetter and Schaeffer, 2001) rather than physical removal. Regardless of the specific mechanisms, this suggests that *n*-alkanes and *n*-alkanoic acids are required at different stages of the growing season and in different amounts.

4.4. Controls on δD of *n*-C_{28} alkanoic acid

For both *n*-alkanes and *n*-alkanoic acids, mean δD_{wax} values were more positive in mature leaves than in late buds (Fig. 2). However, we note that given the same xylem and leaf water and comparable late bud δD_{wax} values, the net D-enrichment of *n*-C_{28} alkanoic acids from buds to mature leaves (44‰) was approximately twice that of *n*-C_{29} alkanes (22‰). We found no relationship between δD_{xw} and $\delta D_{n\text{-C28 acid}}$ ($R^2 = 0.00$, $p = 0.77$), indicating that changes in source water were not influencing $\delta D_{n\text{-C28 acid}}$. Based on correlations, leaf water δD may be a strong driver of *n*-C28 alkanoic acid δD in certain species (*P. serotina*, $R^2 = 0.78$, $p = 0.02$; *Q. alba*, $R^2 = 0.74$, $p = 0.01$; *Q. rubra*, $R^2 = 0.66$, $p = 0.01$) but not in others (*A. saccharinum* and *U. americana*, no correlation).

In mature leaves we found a consistent ~−19‰ offset in the δD values of *n*-C_{29} and *n*-C_{27} alkanes relative to *n*-C_{30} and *n*-C_{28} alkanoic acid, respectively (Fig. 5). Prior calibration studies of mature leaves in temperate biomes found similar $\varepsilon_{alkane/acid}$ offsets of −25‰ in Japan and Thailand (Chikaraishi and Naraoka, 2007) and −30‰ in Massachussettes, USA (Hou et al., 2007). This offset may reflect different D-discrimination during elongation and decarboxylation of the common precursor *n*-alkyl acyl-ACP to produce *n*-alkanoic acids and *n*-alkanes, respectively (Chikaraishi and Naraoka, 2007). Importantly, the systematic negative $\varepsilon_{alkane/acid}$ offset was only observed in mature leaves at BLB. Prior to full leaf expansion we observed positive $\varepsilon_{alkane/acid}$ offsets in all species during the late bud and young leaf stages (Fig. 5). We speculate that the sign change of $\varepsilon_{alkane/acid}$ during the metabolic shift may reflect a change in ε_{bio} from developing leaves that rely on carbohydrate metabolism to mature leaves that rely on current photosynthate. While observations from BLB strengthen the evidence for a systematic $\varepsilon_{alkane/acid}$ offset in temperate settings with relatively low species diversity and a single leaf flush, evidence from locations with exceptionally high species diversity including a tropical forest (Feakins et al., 2016) and botanical garden (Gao et al., 2014) found large interspecies variability in the sign and

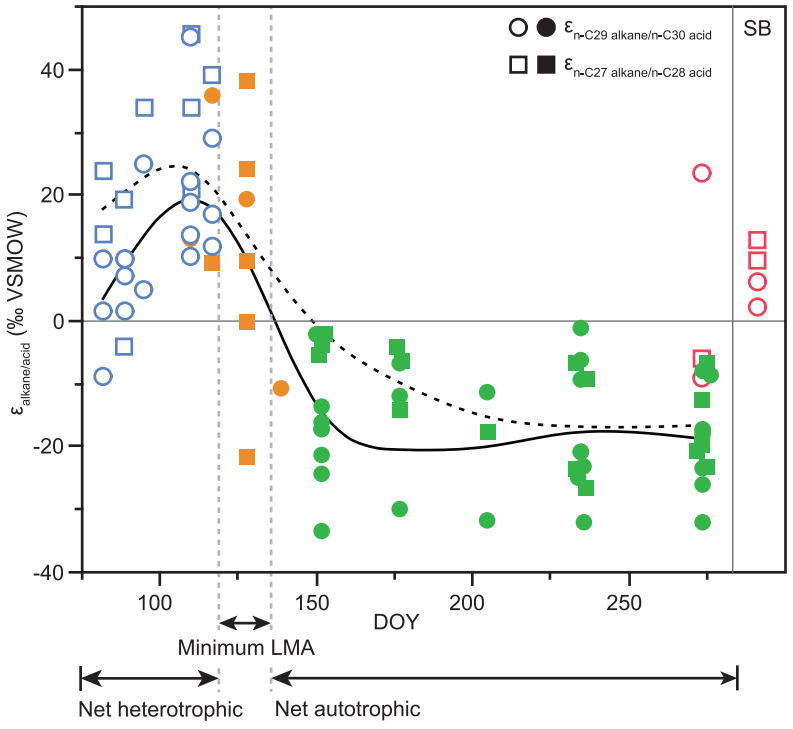

Fig. 5. Fractionation between compound classes, $\varepsilon_{n\text{-C27 alkane}/n\text{-C28 acid}}$ (squares) and $\varepsilon_{n\text{-C29 alkane}/n\text{-C30 acid}}$ (circles). Open symbols represent late buds (blue) and summer buds (red). Closed symbols represent young leaves (orange) and mature leaves (green). Smoothing splines (lambda = 0.05) illustrate general seasonal trends for $\varepsilon_{n\text{-C27 alkane}/n\text{-C28 acid}}$ (dotted line) and $\varepsilon_{n\text{-C29 alkane}/n\text{-C30 acid}}$ (solid line). Dotted vertical lines mark the earliest and latest dates for minimum LMA across all species. Right panel labeled SB includes data from *A. saccharinum* and *Q. rubra* buds collected the following winter. (For interpretation of the references to colour in this figure legend, the reader is referred to the web version of this article.)

magnitude of $\varepsilon_{alkane/acid}$. This suggests that fractionation between compound classes may depend on species diversity and associated heterogeneity in leaf lifespan and the timing of leaf (and leaf wax) development.

4.5. Implications for interpreting δD_{wax} from sediments

Sediments integrate leaf waxes at the regional scale via particulate waxes in aerosols and at the ecosystem scale via direct leaf fall and erosion of soils (Diefendorf and Freimuth, 2017). Here we use observations from BLB to assess the composition and variability of the δD_{wax} signal integrated via direct leaf fall from the tree growth form only. Assuming direct transfer of wax from tree leaf to sediment is a simplification. However, this allows us to estimate the minimum sensitivity of the plant level δD_{wax} signal exclusive of the additional noise likely incorporated at the sediment level by the comprehensive set of wax sources and transport processes.

4.5.1. Interspecies δD_{wax} variability within a growth form

When multiple plant growth forms are present, trees may be a dominant source of long-chain leaf waxes to sediments (Sachse et al., 2012). At BLB, trees have greater spatial coverage and leaf biomass production than other growth forms including grasses, herbs and shrubs. Therefore, we use all tree species to approximate the ecosystem-wide δD_{wax} signal at BLB but acknowledge major differences among species and growth forms with respect to leaf wax ACL and abundance (Diefendorf et al., 2011) and ε_{app} (Sachse et al., 2012) that likely influence wax signals integrated across diverse ecosystems. Relatively low δD_{wax} variability among species just prior to leaf shed (DOY 274) for $\delta D_{n\text{-C29 alkane}}$ (-157 ± 3‰, 1σ) and $\delta D_{n\text{-C28 acid}}$ (-137 ± 7‰, 1σ) suggests that the community-integrated δD_{wax} signal will not be weighted toward those species with the highest wax concentration, leaf biomass production or abundance within the forest. This may not be the case for sites with greater interspecies δD_{wax} variability. A comparison with $\delta D_{n\text{-C29 alkane}}$ reported from other deciduous angiosperm tree species sampled at temperate sites from August through November indicates that the interspecies $\delta D_{n\text{-C29 alkane}}$ variability at BLB from August-October ($1\sigma = 5$‰, $n = 5$ species) is less than half that observed at other sites (Fig. 6). For instance, variability for 9 tree species at Blood Pond, Massachusetts was 11‰ (Hou et al., 2007). When including all growth forms at the same site, interspecies variability rose to 65‰. Even within a species, variability can be relatively high, for example 15‰ among 3 biological replicates of the woody shrub *Corylus americana* sampled in October in Connecticut (Oakes and Hren, 2016). Biological δD_{wax} variability at a single site and even within a single growth form (trees) potentially limits the sensitivity of ecosystem-integrated δD_{wax} records to changes in δD_p that are greater in magnitude than interspecies variability (i.e., 5‰ at BLB, 11‰ at Blood Pond, Massachusetts). However, we note that the full range of δD_{wax} variability among growth forms

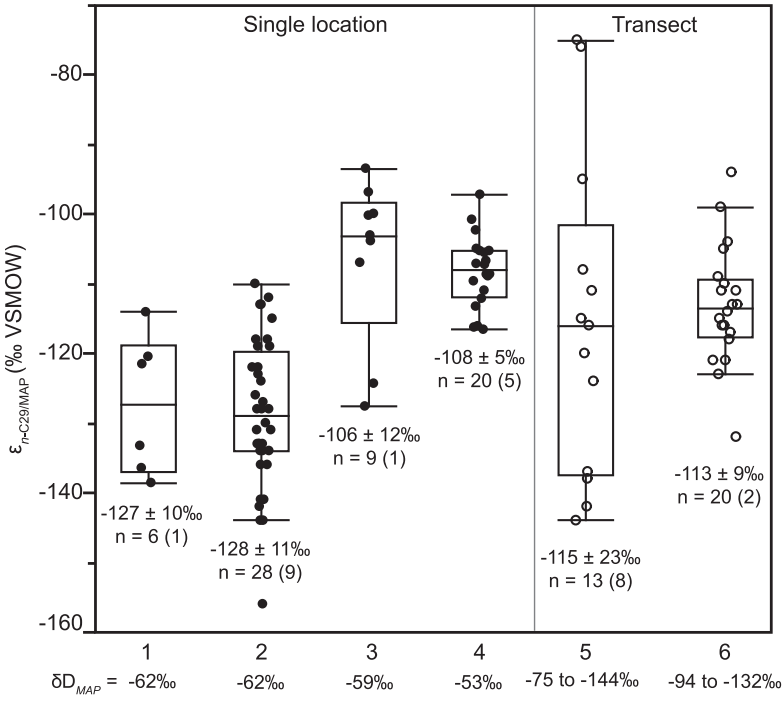

Fig. 6. Comparison of $\varepsilon_{n\text{-C29/MAP}}$ observed in this study with comparable published data from deciduous angiosperm trees and woody shrubs sampled in temperate biomes during the mature leaf stage, August to November. Panels include data from single locations (closed symbols); and from transect studies (open symbols). Data are numbered by study as follows: (1) Sachse et al. (2009) (*Acer pseudoplatanus* only); (2) Hou et al. (2007); (3) Oakes and Hren (2016); (4) this study; (5) Sachse et al. (2006); (6) Tipple and Pagani (2013). The OIPC modeled δD_{MAP} for the sites(s) of sample collection are listed below each study number. Mean $\varepsilon_{n\text{-C29/MAP}}$ values $\pm 1\sigma$, and the number of individuals and species (in parentheses) appear below each boxplot.

and species within a site may increase these thresholds considerably. This complicates selection of accurate ε_{app} values for interpretation of sedimentary δD_{wax} and demonstrates the need to understand how biological noise is integrated at the sediment level.

4.5.2. n-Alkanes and n-alkanoic acids record different source water information

We observed several key differences among compound classes that may support the use of either *n*-alkanes or *n*-alkanoic acids for paleohydrology applications. First, we found that *n*-alkane concentrations in mature leaves were 1.5–20 times higher than *n*-alkanoic acid concentrations in the same species, except for *U. americana* where *n*-alkane concentrations were ~20% lower than *n*-alkanoic acids. Therefore, we anticipate that *n*-alkanes will be several times more abundant in the ecosystem-integrated wax than *n*-alkanoic acids, ignoring potential differences in preservation among compound classes. Based on higher interspecies concentration differences for *n*-alkanes ($1\sigma = 1020$ μg/g dry leaf) than for *n*-alkanoic acids ($1\sigma = 123$ μg/g dry leaf), there is higher potential for weighting of the ecosystem-integrated signal toward species with highest *n*-alkane concentrations.

Second, $\varepsilon_{n\text{-C29/xw}}$ and $\varepsilon_{n\text{-C28/xw}}$ values stabilized early in the mature leaf stage (by DOY 177 and 152, respectively), after which *n*-C_{29} alkane synthesis ceased and *n*-C_{28} synthesis continued (Fig. 2, Table 1). Therefore, at BLB and other sites where source water δD is stable through the growing season (i.e., $\delta D_{xw} = \delta D_{MAP}$; Fig. 1), ε_{app} is likely set for both compound classes at the onset of leaf maturity, regardless of wax production or loss in mature leaves. However, for conditions in which δD_{xw} changes in response to short term (monthly to seasonal) δD_p variations, continued synthesis of *n*-alkanoic acids through the growing season could potentially bias $\delta D_{n\text{-C28 acid}}$ records toward summer and autumn source water δD. These conditions could include sites with abundant and reliable summer rainfall (Ehleringer and Dawson, 1992), plants with shallow rooting depths or with DBH < ~12 cm (Dawson and Ehleringer, 1991; Phillips and Ehleringer, 1995), coastal plants influenced by changing source water salinity, trees with limited access to groundwater (White et al., 1985), riparian plants using ephemeral stream water, or annuals and herbaceous plants more likely to use summer precipitation than woody plants (Ehleringer et al., 1991).

Third, we observed that toward the end of the mature leaf stage (DOY 235–274) interspecies $\delta D_{n\text{-C28 acid}}$ variability was ~2–3 times that of $\delta D_{n\text{-C29 alkane}}$ (Table 1). Higher interspecies δD variability in *n*-alkanoic acids relative to *n*-alkanes has been observed previously (Chikaraishi and Naraoka, 2007; Hou et al., 2007; Feakins et al., 2016). This may result in reduced biological noise in $\delta D_{n\text{-C29 alkane}}$ relative to $\delta D_{n\text{-C28 acid}}$ sedimentary records, and thus greater precision for reconstructing δD_p $\delta D_{n\text{-C29 alkane}}$. Finally, we found that ε_{app} values in mature leaves were consistently ~19‰ more positive for *n*-acids than for *n*-alkanes (Fig. 5), similar to prior observations in temperate settings (Chikaraishi and Naraoka, 2007; Hou et al., 2007). The majority of calibrations of ε_{app} in modern vegetation have been developed for *n*-alkanes and therefore may not be appropriate to apply to reconstructions of past δD_p using *n*-alkanoic acids in sediments. A more comprehensive calibration dataset may be needed for robust estimates of ε_{app} values specific to *n*-alkanoic acids.

4.5.3. Estimating ε_{app} values and uncertainty

ε_{app} remains the largest source of uncertainty in leaf wax paleohydrology (Sachse et al., 2012; Polissar and D'Andrea, 2014). Even within the same growth form and biome there can be considerable site-to-site variation in ε_{app} (Fig. 6). Thus, applying ε_{app} values determined at other sites to interpret sedimentary δD_{wax} may introduce additional uncertainty into δD_p reconstructions. Conversely, site-specific ε_{app} calibrations based on modern vegetation may have limited accuracy for downcore δD_{wax} interpretation, especially during past ecologic transitions or periods when ancient plant communities were significantly different from the modern.

Hydrogen isotope data from BLB provide an opportunity to quantify the propagated analytical uncertainty in leaf wax and source water δD values and estimate the total uncertainty in resulting ε_{app} at the level of the growth form (i.e., trees). We estimate that the error propagated uncertainty in our measured ε_{app} values is 6.7‰ (1σ) for $\varepsilon_{n\text{-C29/MAP}}$ and 6.9‰ (1σ) for $\varepsilon_{n\text{-C28/MAP}}$. This was calculated using a Monte Carlo simulation with 10,000 iterations (e.g., Anderson, 1976) of the weighted mean 1σ for the measured δD_{wax} of all species and individuals during the mature leaf stage, as well as the 95% confidence interval (4‰) reported for the modeled δD_{MAP} value at BLB (OIPC, Bowen and Revenaugh, 2003; Bowen, 2015). The same simulation using the weighted mean 1σ of measured δD_{xw} as the source water input estimates a slightly higher uncertainty for $\varepsilon_{n\text{-C29/xw}}$ (8.7‰) and $\varepsilon_{n\text{-C28/xw}}$ (8.8‰). Therefore, the total uncertainty in ε_{app} estimates based on all species within a single growth form (trees) at BLB is approximately 9‰. While this is considerably lower than other conservative estimates of ε_{app} uncertainty (~25‰; Polissar and D'Andrea, 2014), we note that ε_{app} uncertainty would likely increase with inclusion of multiple growth forms at the sediment level. Therefore we consider 9‰ to be a minimum expected uncertainty in ecosystem-integrated ε_{app} values at BLB, which may be similar for other temperate sites. Additional factors including the transport and integration of leaf waxes in sediments and ecological changes through time likely further affect the uncertainty of ε_{app} estimates applied to sedimentary records.

5. CONCLUSIONS

We provide a record of seasonal changes in the δD composition of *n*-alkanes and *n*-alkanoic acids and plant source waters for five tree species growing in a temperate deciduous forest. This dataset allows us to approximate the δD_{wax} signal integrated across the tree growth form, which may have a strong influence on sedimentary δD_{wax} records. Results indicate that long chain *n*-alkanes and *n*-alkanoic acids produced in the same plant differ in key ways including concentration, timing of synthesis and δD composition. Specifically, in four out of five tree species, *n*-alkane concentrations in mature leaves were 2–29 times higher

than *n*-alkanoic acid concentrations in the same individuals. Further, while the majority of *de novo* *n*-C_{29} alkane synthesis occurs during a discrete interval as leaves reach full expansion (24–35 days after leaf emergence), *n*-C_{28} alkanoic acids are produced throughout the growing season. Bulk leaf $\delta^{13}C$ suggests that phenologic development controls the timing and amount of *n*-alkanes produced. During leaf emergence and expansion, exposure of leaf tissues with immature cuticle appears to drive a strong transpirational D-enrichment of leaf water which, in turn, acts as a primary control on δD_{wax} values as leaves and the cuticle reach maturity. Despite differences in the timing of *n*-alkane and *n*-alkanoic acid synthesis, δD_{wax} values for both compound classes are primarily determined during the period of leaf emergence and expansion. This suggests that the δD_{wax} signal from trees in temperate settings may be biased toward the local timing of spring leaf emergence. A secondary control on δD_{wax} may be a shift in plant metabolism and the δD composition of H used for wax synthesis in developing and mature leaves.

Prior to autumn leaf fall, interspecies $\delta D_{n\text{-C29 alkane}}$ variability ($1\sigma = 4‰$) was lower than for $\delta D_{n\text{-C28 acid}}$ ($1\sigma = 9‰$), suggesting that *n*-alkanes may be more precise tracers of changes in source water δD. During the mature leaf stage we observed a consistent $\sim -19‰$ offset of $\varepsilon_{n\text{-C29/xw}}$ values relative to $\varepsilon_{n\text{-C28/xw}}$, underscoring that the two compound classes fractionate shared source water to different extents and should be interpreted from sedimentary records accordingly. Overall, these data suggest that the distinct abundance, timing of synthesis and ε_{app} values of *n*-alkanes and *n*-alkanoic acids merit consideration when applying either as paleohydrology proxies.

ACKNOWLEDGEMENTS

We thank Michael Hren, two anonymous reviewers and Associate Editor Alex Sessions for their helpful suggestions to improve this manuscript. Thanks go to Dr. Gregory Wiles, Nicholas Wiesenberg and Douglas Sberna for sample collection assistance and to The Nature Conservancy for site access. This research was supported by the National Science Foundation (EAR-1229114 to AFD). Acknowledgment is made to the Donors of the American Chemical Society Petroleum Research Fund for partial support of this research (PRF #51787-DNI2 to AFD). Fieldwork was supported by a grant from the American Philosophical Society to EJF. This research was also supported by awards from the Geological Society of America and SigmaXi to EJF.

APPENDIX A. SUPPLEMENTARY MATERIAL

Supplementary data associated with this article can be found, in the online version, at http://dx.doi.org/10.1016/j.gca.2017.02.027.

REFERENCES

Baker E. and Hunt G. M. (1981) Developmental changes in leaf epicuticular waxes in relation to foliar penetration. *New Phytol.* **88**, 731–747.

Bush R. T. and McInerney F. A. (2013) Leaf wax *n*-alkane distributions in and across modern plants: implications for paleoecology and chemotaxonomy. *Geochim. Cosmochim. Acta* **117**, 161–179.

Bowen G. J. and Revenaugh J. (2003) Interpolating the isotopic composition of modern meteoric precipitation. *Water Resour. Res.* **39**, 1299.

Bowen, G. J. (2015) The Online Isotopes in Precipitation Calculator, version 2.2. http://www.waterisotopes.org.

Cernusak L., Pate J. S. and Farquhar G. (2002) Diurnal variation in the stable isotope composition of water and dry matter in fruiting Lupinus angustifolius under field conditions. *Plant, Cell Environ.* **25**, 893–907.

Cernusak L. A., Tcherkez G., Keitel C., Cornwell W. K., Santiago L. S., Knohl A., Barbour M. M., Williams D. G., Reich P. B., Ellsworth D. S., Dawson T. E., Griffiths H. G., Farquhar G. D. and Wright I. J. (2009) Why are non-photosynthetic tissues generally ^{13}C enriched compared with leaves in C3 plants? Review and synthesis of current hypotheses. *Funct. Plant Biol.* **36**, 199–213.

Cernusak L. A., Barbour M. M., Arndt S. K., Cheesman A. W., English N. B., Feild T. S., Helliker B. R., Holloway-Phillips M. M., Holtum J. A. and Kahmen A. (2015) Stable isotopes in leaf water of terrestrial plants. *Plant, Cell Environ.*.

Chikaraishi Y. and Naraoka H. (2007) $\Delta^{13}C$ and δD relationships among three n-alkyl compound classes (*n*-alkanoic acid, *n*-alkane and *n*-alkanol) of terrestrial higher plants. *Org. Geochem.* **38**, 198–215.

Collier D. E. and Thibodeau B. A. (1995) Changes in respiration and chemical content during autumnal senescence of Populus tremuloides and Quercus rubra leaves. *Tree Physiol.* **15**, 759–764.

Constable G. and Rawson H. (1980) Effect of leaf position, expansion and age on photosynthesis, transpiration and water use efficiency of cotton. *Funct. Plant Biol.* **7**, 89–100.

Coplen T. B., Brand W. A., Gehre M., Gröning M., Meijer H. A. J., Toman B. and Verkouteren R. M. (2006) New guidelines for $\delta^{13}C$ measurements. *Anal. Chem.* **78**, 2439–2441.

Cornelissen J. H. C., Lavorel S., Garnier E., Diaz S., Buchmann N., Gurvich D. E., Reich P. B., Steege H. t., Morgan H. D., Heijden M. G. A. v. d., Pausas J. G. and Poorter H. (2003) A handbook of protocols for standardised and easy measurement of plant functional traits worldwide. *Aust. J. Bot.* **51**, 335–380.

Craig H. (1961) Isotopic variations in meteoric waters. *Science* **133**, 1702–1703.

Damesin C., Rambal S. and Joffre R. (1998) Seasonal and annual changes in leaf δ13C in two co-occurring Mediterranean oaks: relations to leaf growth and drought progression. *Funct. Ecol.* **12**, 778–785.

Damesin C. and Lelarge C. (2003) Carbon isotope composition of current-year shoots from Fagus sylvatica in relation to growth, respiration and use of reserves. *Plant, Cell Environ.* **26**, 207–219.

Dawson T. E. and Ehleringer J. R. (1991) Streamside trees that do not use stream water. *Nature* **350**, 335–337.

Dawson T. E. and Ehleringer J. R. (1993) Isotopic enrichment of water in the "woody" tissues of plants: implications for plant water source, water uptake, and other studies which use the stable isotopic composition of cellulose. *Geochim. Cosmochim. Acta* **57**, 3487–3492.

Dawson T. E., Mambelli S., Plamboeck A. G., Templer P. H. and Tu K. P. (2002) Stable isotopes in plant ecology. *Annu. Rev. Ecol. Syst.* **33**, 507–559.

Diefendorf A. F., Freeman K. H., Wing S. L. and Graham H. V. (2011) Production of *n*-alkyl lipids in living plants and implications for the geologic past. *Geochim. Cosmochim. Acta* **75**, 7472–7485.

Diefendorf A. F. and Freimuth E. J. (2017) Extracting the most from terrestrial plant-derived n-alkyl lipids and their carbon

isotopes from the sedimentary record: a review. *Org. Geochem.* **103**, 1–21.
Eglinton G. and Hamilton R. J. (1967) Leaf epicuticular waxes. *Science* **156**, 1322–1335.
Ehleringer J. R., Phillips S. L., Schuster W. S. and Sandquist D. R. (1991) Differential utilization of summer rains by desert plants. *Oecologia* **88**, 430–434.
Ehleringer J. and Dawson T. (1992) Water uptake by plants: perspectives from stable isotope composition. *Plant, Cell Environ.* **15**, 1073–1082.
Eley Y., Dawson L., Black S., Andrews J. and Pedentchouk N. (2014) Understanding 2H/1H systematics of leaf wax n-alkanes in coastal plants at Stiffkey saltmarsh, Norfolk, UK. *Geochim. Cosmochim. Acta* **128**, 13–28.
Ellsworth D. and Reich P. (1993) Canopy structure and vertical patterns of photosynthesis and related leaf traits in a deciduous forest. *Oecologia* **96**, 169–178.
Feakins S. J. and Sessions A. L. (2010) Controls on the D/H ratios of plant leaf waxes from an arid ecosystem. *Geochim. Cosmochim. Acta* **74**, 2128–2141.
Feakins S. J., Bentley L. P., Salinas N., Shenkin A., Blonder B., Goldsmith G. R., Ponton C., Arvin L. J., Wu M. S. and Peters T. (2016) Plant leaf wax biomarkers capture gradients in hydrogen isotopes of precipitation from the Andes and Amazon. *Geochim. Cosmochim. Acta* **182**, 155–172.
Gamarra B. and Kahmen A. (2015) Concentrations and δ2H values of cuticular n-alkanes vary significantly among plant organs, species and habitats in grasses from an alpine and a temperate European grassland. *Oecologia* **178**, 981–998.
Gao L., Edwards E. J., Zeng Y. and Huang Y. (2014) Major evolutionary trends in hydrogen isotope fractionation of vascular plant leaf waxes. *PLoS One* **9**, e112610.
Graham H. V., Patzkowsky M. E., Wing S. L., Parker G. G., Fogel M. L. and Freeman K. H. (2014) Isotopic characteristics of canopies in simulated leaf assemblages. *Geochim. Cosmochim. Acta* **144**, 82–95.
Hauke V. and Schreiber L. (1998) Ontogenetic and seasonal development of wax composition and cuticular transpiration of ivy (Hedera helix L.) sun and shade leaves. *Planta* **207**, 67–75.
Helliker B. R., Roden J. S., Cook C. and Ehleringer J. R. (2002) A rapid and precise method for sampling and determining the oxygen isotope ratio of atmospheric water vapor. *Rapid Commun. Mass Spectrom.* **16**, 929–932.
Hou J. Z., D'Andrea W. J., MacDonald D. and Huang Y. S. (2007) Hydrogen isotopic variability in leaf waxes among terrestrial and aquatic plants around Blood Pond, Massachusetts (USA). *Org. Geochem.* **38**, 977–984.
Hou J., D'Andrea W. J. and Huang Y. (2008) Can sedimentary leaf waxes record D/H ratios of continental precipitation? Field, model, and experimental assessments. *Geochim. Cosmochim. Acta* **72**, 3503–3517.
Jetter R. and Schaeffer S. (2001) Chemical composition of the *Prunus laurocerasus* leaf surface. Dynamic changes of the epicuticular wax film during leaf development. *Plant Physiol.* **126**, 1725–1737.
Jetter R., Kunst L. and Samuels A. L. (2006) Composition of plant cuticular waxes. In *Biology of the plant cuticle* (eds. M. Rieder and C. Muller). Blackwell Publishing, Oxford, pp. 145–181.
Kahmen A., Hoffmann B., Schefuß E., Arndt S. K., Cernusak L. A., West J. B. and Sachse D. (2013a) Leaf water deuterium enrichment shapes leaf wax *n*-alkane δD values of angiosperm plants II: Observational evidence and global implications. *Geochim. Cosmochim. Acta* **111**, 50–63.
Kahmen A., Schefuß E. and Sachse D. (2013b) Leaf water deuterium enrichment shapes leaf wax n-alkane δD values of angiosperm plants I: Experimental evidence and mechanistic insights. *Geochim. Cosmochim. Acta* **111**, 39–49.
Kaplan J. O., Prentice I. C. and Buchmann N. (2002) The stable carbon isotope composition of the terrestrial biosphere: modeling at scales from the leaf to the globe. *Global Biogeochem. Cycles* **16**, 1060.
Kunst L., Jetter R. and Samuels A. L. (2008) Biosynthesis and transport of plant cuticular waxes. *Ann. Plant Rev.* **23**, 182–215.
Leavitt S. W. and Long A. (1985) Stable-carbon isotopic composition of maple sap and foliage. *Plant Physiol.* **78**, 427–429.
Lechowicz M. J. (1984) Why do temperate deciduous trees leaf out at different times? Adaptation and ecology of forest communities. *Am. Naturalist* **124**, 821–842.
Maycock P. F. (1961) Botanical studies on Mont St. Hilaire, Rouville County, Quebec. *Can. J. Bot.* **39**, 1293–1325.
McInerney F. A., Helliker B. R. and Freeman K. H. (2011) Hydrogen isotope ratios of leaf wax n-alkanes in grasses are insensitive to transpiration. *Geochim. Cosmochim. Acta* **75**, 541–554.
McKown A. D., Guy R. D., Azam M. S., Drewes E. C. and Quamme L. K. (2013) Seasonality and phenology alter functional leaf traits. *Oecologia* **172**, 653–665.
Newberry S. L., Kahmen A., Dennis P. and Grant A. (2015) *N*-Alkane biosynthetic hydrogen isotope fractionation is not constant throughout the growing season in the riparian tree *Salix viminalis*. *Geochim. Cosmochim. Acta* **165**, 75–85.
Niinemets Ü. and Tenhunen J. (1997) A model separating leaf structural and physiological effects on carbon gain along light gradients for the shade-tolerant species Acer saccharum. *Plant, Cell Environ.* **20**, 845–866.
Niinemets Ü. (1999) Research review. Components of leaf dry mass per area–thickness and density–alter leaf photosynthetic capacity in reverse directions in woody plants. *New Phytol.* **144**, 35–47.
Oakes A. M. and Hren M. T. (2016) Temporal variations in the δD of leaf n-alkanes from four riparian plant species. *Org. Geochem.* **97**, 122–130.
Pagani M., Pedentchouk N., Huber M., Sluijs A., Schouten S., Brinkhuis H., Damsté J. S. S., Dickens G. R., Backman J. and Clemens S. (2006) Arctic hydrology during global warming at the palaeocene/eocene thermal maximum. *Nature* **442**, 671–675.
Pantin F., Simonneau T., Rolland G., Dauzat M. and Muller B. (2011) Control of leaf expansion: a developmental switch from metabolics to hydraulics. *Plant Physiol.* **156**, 803–815.
Pantin F., Simonneau T. and Muller B. (2012) Coming of leaf age: control of growth by hydraulics and metabolics during leaf ontogeny. *New Phytol.* **196**, 349–366.
Phillips S. L. and Ehleringer J. R. (1995) Limited uptake of summer precipitation by bigtooth maple (Acer grandidentatum Nutt) and Gambel's oak (Quereus gambelii Nutt). *Trees* **9**, 214–219.
Piasentier E., Bovolenta S. and Malossini F. (2000) The n-alkane concentrations in buds and leaves of browsed broadleaf trees. *J. Agric. Sci.* **135**, 311–320.
Polissar P. J. and Freeman K. H. (2010) Effects of aridity and vegetation on plant-wax δD in modern lake sediments. *Geochim. Cosmochim. Acta* **74**, 5785–5797.
Polissar P. J. and D'Andrea W. J. (2014) Uncertainty in paleohydrologic reconstructions from molecular δD values. *Geochim. Cosmochim. Acta* **129**, 146–156.
Poorter H., Niinemets U., Poorter L., Wright I. J. and Villar R. (2009) Causes and consequences of variation in leaf mass per area (LMA): a meta-analysis. *New Phytol.* **182**, 565–588.
Rach O., Brauer A., Wilkes H. and Sachse D. (2014) Delayed hydrological response to Greenland cooling at the onset of the Younger Dryas in western Europe. *Nat. Geosci.* **7**, 109–112.

Riederer M. and Schreiber L. (2001) Protecting against water loss: analysis of the barrier properties of plant cuticles. *J. Exp. Bot.* **52**, 2023–2032.

Roden J. S., Lin G. and Ehleringer J. R. (2000) A mechanistic model for interpretation of hydrogen and oxygen isotope ratios in tree-ring cellulose. *Geochim. Cosmochim. Acta* **64**, 21–35.

Sachse D., Radke J. and Gleixner G. (2004) Hydrogen isotope ratios of recent lacustrine sedimentary n-alkanes record modern climate variability. *Geochim. Cosmochim. Acta* **68**, 4877–4889.

Sachse D., Radke J. and Gleixner G. (2006) ΔD values of individual *n*-alkanes from terrestrial plants along a climatic gradient – implications for the sedimentary biomarker record. *Org. Geochem.* **37**, 469–483.

Sachse D., Kahmen A. and Gleixner G. (2009) Significant seasonal variation in the hydrogen isotopic composition of leaf-wax lipids for two deciduous tree ecosystems (*Fagus sylvativa* and *Acer pseudoplatanus*). *Org. Geochem.* **40**, 732–742.

Sachse D., Gleixner G., Wilkes H. and Kahmen A. (2010) Leaf wax *n*-alkane δD values of field-grown barley reflect leaf water δD values at the time of leaf formation. *Geochim. Cosmochim. Acta* **74**, 6741–6750.

Sachse D., Billault I., Bowen G. J., Chikaraishi Y., Dawson T. E., Feakins S. J., Freeman K. H., Magill C. R., McInerney F. A., van der Meer M. T. J., Polissar P., Robins R. J., Sachs J. P., Schmidt H.-L., Sessions A. L., White J. W. C., West J. B. and Kahmen A. (2012) Molecular paleohydrology: interpreting the hydrogen-isotopic composition of lipid biomarkers from photosynthesizing organisms. *Ann. Rev. Earth Planet. Sci.* **40**, 221–249.

Sachse D., Dawson T. E. and Kahmen A. (2015) Seasonal variation of leaf wax n-alkane production and δ2H values from the evergreen oak tree, Quercus agrifolia. *Isotopes Environ. Health Stud.* **51**, 124–142.

Schmidt H.-L., Werner R. A. and Eisenreich W. (2003) Systematics of 2H patterns in natural compounds and its importance for the elucidation of biosynthetic pathways. *Phytochem. Rev.* **2**, 61–85.

Schwab V. F., Garcin Y., Sachse D., Todou G., Séné O., Onana J.-M., Achoundong G. and Gleixner G. (2015) Effect of aridity on $\delta^{13}C$ and δD values of C_3 plant- and C_4 graminoid-derived leaf wax lipids from soils along an environmental gradient in Cameroon (Western Central Africa). *Org. Geochem.* **78**, 99–109.

Seki O., Nakatsuka T., Shibata H. and Kawamura K. (2010) A compound-specific n-alkane $\delta^{13}C$ and δD approach for assessing source and delivery processes of terrestrial organic matter within a forested watershed in northern Japan. *Geochim. Cosmochim. Acta* **74**, 599–613.

Sessions A. L., Burgoyne T. W., Schimmelmann A. and Hayes J. M. (1999) Fractionation of hydrogen isotopes in lipid biosynthesis. *Org. Geochem.* **30**, 1193–1200.

Sessions A. L. (2006) Seasonal changes in D/H fractionation accompanying lipid biosynthesis in *Spartina alterniflora*. *Geochim. Cosmochim. Acta* **70**, 2153–2162.

Shepherd T. and Griffiths D. W. (2006) The effects of stress on plant cuticular waxes. *New Phytol.* **171**, 469–499.

Smith F. A. and Freeman K. H. (2006) Influence of physiology and climate on δD of leaf wax n-alkanes from C3 and C4 grasses. *Geochim. Cosmochim. Acta* **70**, 1172–1187.

Song X., Barbour M. M., Farquhar G. D., Vann D. R. and Helliker B. R. (2013) Transpiration rate relates to within-and across-species variations in effective path length in a leaf water model of oxygen isotope enrichment. *Plant, Cell Environ.* **36**, 1338–1351.

Tierney J. E., Russell J. M., Huang Y., Damsté J. S. S., Hopmans E. C. and Cohen A. S. (2008) Northern hemisphere controls on tropical southeast African climate during the past 60,000 years. *Science* **322**, 252–255.

Tipple B. J., Berke M. A., Doman C. E., Khachaturyan S. and Ehleringer J. R. (2013) Leaf-wax *n*-alkanes record the plant–water environment at leaf flush. *Proc. Natl. Acad. Sci.* **110**, 2659–2664.

Tipple B. J. and Pagani M. (2013) Environmental control on eastern broadleaf forest species' leaf wax distributions and D/H ratios. *Geochim. Cosmochim. Acta* **111**, 64–77.

Tipple B. J., Berke M. A., Hambach B., Roden J. S. and Ehleringer J. R. (2015) Predicting leaf wax n-alkane 2H/1H ratios: controlled water source and humidity experiments with hydroponically grown trees confirm predictions of Craig-Gordon model. *Plant, Cell Environ.* **38**, 1035–1047.

Turgeon R. (1989) The sink-source transition in leaves. *Annu. Rev. Plant Biol.* **40**, 119–138.

Wesołowski T. and Rowiński P. (2006) Timing of bud burst and tree-leaf development in a multispecies temperate forest. *For. Ecol. Manage.* **237**, 387–393.

West A. G., Patrickson S. J. and Ehleringer J. R. (2006) Water extraction times for plant and soil materials used in stable isotope analysis. *Rapid Commun. Mass Spectrom.* **20**, 1317–1321.

White J. W., Cook E. R. and Lawrence J. R. (1985) The DH ratios of sap in trees: Implications for water sources and tree ring DH ratios. *Geochim. Cosmochim. Acta* **49**, 237–246.

Wright I. J., Reich P. B., Westoby M., Ackerly D. D., Baruch Z., Bongers F., Cavender-Bares J., Chapin T., Cornelissen J. H. C., Diemer M., Flexas J., Garnier E., Groom P. K., Gulias J., Hikosaka K., Lamont B. B., Lee T., Lee W., Lusk C., Midgley J. J., Navas M.-L., Niinemets U., Oleksyn J., Osada N., Poorter H., Poot P., Prior L., Pyankov V. I., Roumet C., Thomas S. C., Tjoelker M. G., Veneklaas E. J. and Villar R. (2004) The worldwide leaf economics spectrum. *Nature* **428**, 821–827.

Associate editor: Alex L Sessions